

1 **Seasonality of isoprenoid emissions from a primary rainforest in central Amazonia**

2 *E. G. Alves (1), K. Jardine (2), J. Tota (3), A. Jardine (1), A. M. Yáñez-Serrano(1,4), T.*

3 *Karl (5), J. Tavares (6), B. Nelson (6), D. Gu (7), T. Stavrakou (8), S. Martin (9), P. Artaxo*

4 *(10), A. Manzi (1,11), and A. Guenther (7).*

5 (1) Climate and Environment Department, National Institute for Amazonian Research
6 (INPA) and State University of Amazonas (UEA), Av. André Araújo 2936, CEP 69067-
7 375, Manaus-AM, Brazil

8 (2) Climate Science Department, Earth Science Division, Lawrence Berkeley National
9 Laboratory (LBNL), One Cyclotron Rd, building 64-241, Berkeley, CA 94720, USA.

10 (3) Institute of Engineering and Geoscience, Federal University of West Para (UFOPA),
11 Rua Vera Paz s/n, CEP 68035-110, Santarem-PA, Brazil.

12 (4) Biogeochemistry Department, Max Planck Institute for Chemistry, P. O. Box 3060,
13 55128, Mainz, Germany.

14 (5) Institute for Meteorology and Geophysics, University of Innsbruck, Innrain 52, A-6020,
15 Innsbruck, Austria.

16 (6) Ecology Department, National Institute for Amazonian Research (INPA), Av. André
17 Araújo 2936, CEP 69067-375, Manaus-AM, Brazil

18 (7) Department of Earth System Science, University of California, Irvine, USA.

19 (8) Belgian Institute for Space Aeronomy, Avenue Circulaire 3, 1180 Uccle, Brussels,
20 Belgium.

21 (9) School of Engineering and Applied Sciences, Department of Earth and Planetary
22 Sciences, Harvard University, 29 Oxford St ,Cambridge, MA 02138, USA.

23 (10) Institute of Physics, University of Sao Paulo, Rua Matão, Travessa R, 187 – Cidade
24 Universitária, CEP 05508-900, Sao Paulo-SP, Brazil.

25 (11) National Institute for Spatial Research, Center of Weather Forecasting and Climate
26 Studies, Rod. Presidente Dutra, km 40, Cachoeira Paulista/SP

27 Correspondence to: elianegomes.alves@gmail.com

28

29 **Abstract**

30 Tropical rainforests are an important source of isoprenoid and other Volatile Organic
31 Compound (VOC) emissions to the atmosphere. The seasonal variation of these compounds
32 is however still poorly understood. In this study, vertical profiles of mixing ratios of
33 isoprene, total monoterpenes and total sesquiterpenes, were measured within and above the
34 canopy, in a primary rainforest in central Amazonia, using a Proton Transfer Reaction –
35 Mass Spectrometer (PTR-MS). Fluxes of these compounds from the canopy into the
36 atmosphere were estimated from PTR-MS measurements by using an inverse Lagrangian
37 transport model. Measurements were carried out continuously from September 2010 to
38 January 2011, encompassing the dry and wet seasons. Mixing ratios were higher during the
39 dry (isoprene – 2.68 ± 0.9 ppbv, total monoterpenes - 0.67 ± 0.3 ppbv; total sesquiterpenes –
40 0.09 ± 0.07 ppbv) than the wet season (isoprene – 1.66 ± 0.9 ppbv, total monoterpenes -
41 0.47 ± 0.2 ppbv; total sesquiterpenes - 0.03 ± 0.02 ppbv) for all compounds. Ambient air
42 temperature and photosynthetically active radiation (PAR) behaved similarly. Daytime
43 isoprene and total monoterpene mixing ratios were highest within the canopy, rather than
44 near the ground or above the canopy. By comparison, daytime total sesquiterpene mixing
45 ratios were highest near the ground. Daytime fluxes varied significantly between seasons
46 for all compounds. The maximums for isoprene ($2.53 \pm 0.5 \mu\text{mol m}^{-2} \text{h}^{-1}$) and total
47 monoterpenes ($1.77 \pm 0.05 \mu\text{mol m}^{-2} \text{h}^{-1}$) were observed in the late dry season, whereas the
48 maximum for total sesquiterpenes was found during the dry-to-wet transition season
49 ($0.77 \pm 0.1 \mu\text{mol m}^{-2} \text{h}^{-1}$). These flux estimates suggest that the canopy is the main source of
50 isoprenoids emitted into the atmosphere for all seasons. However, uncertainties in
51 turbulence parameterization near the ground could affect estimates of fluxes that come from
52 the ground. Leaf phenology seemed to be an important driver of seasonal variation of
53 isoprenoid emissions. Although remote sensing observations of changes in leaf area index
54 were used to estimate leaf phenology, MEGAN 2.1 did not fully capture the behavior of
55 seasonal emissions observed in this study. This could be a result of very local effects on the
56 observed emissions, but also suggest that other parameters need to be better determined in
57 Biogenic Volatile Organic Compound (BVOC) models. Our results support established
58 findings that seasonality of isoprenoids are driven by seasonal changes in light, temperature
59 and leaf phenology. However, they suggest that leaf phenology and its role on isoprenoid

60 production and emission from tropical plant species needs to be better understood in order
61 to develop mechanistic explanations for seasonal variation in emissions. This also may
62 reduce the uncertainties of model estimates associated with the responses to environmental
63 factors. Therefore, this study strongly encourages long-term measurements of isoprenoid
64 emissions, environmental factors and leaf phenology from leaf to ecosystem scale, with the
65 purpose of improving BVOC model approaches that can characterize seasonality of
66 isoprenoid emissions from tropical rainforests.

67

68 **Key-words:** Isoprene, monoterpenes, sesquiterpenes, leaf phenology, seasonal changes

69

70 **1. Introduction**

71 Terrestrial vegetation emits high quantities of biogenic volatile organic compounds
72 (BVOCs) to the atmosphere (Guenther et al., 2006, 2012), which are removed by oxidation
73 reactions, deposition of reaction products (Lelieveld et al., 2008) and consumption by
74 surfaces (Gray et al., 2014). Emissions and subsequent transformations in the atmosphere
75 have been widely explored by the scientific community. However, there is still a need for
76 improving our understanding of how BVOC emissions and their reaction products vary
77 seasonally and are involved in atmosphere chemistry, biogeochemical cycling and climate
78 at local, regional and global scales.

79 Despite a large number of BVOC species that have been identified within plants and
80 in emissions from plants, the largest part of the global biogenic emissions and subsequent
81 effect on atmospheric chemistry are thought to be associated with isoprenoids
82 (Laothawornkitkul et al., 2009). The isoprenoids are an important class of organic
83 compounds that include isoprene (containing five carbon atoms - C₅), monoterpenes (10
84 carbon atoms - C₁₀), sesquiterpenes (15 carbon atoms - C₁₅) and diterpenes (20 carbon
85 atoms - C₂₀) (Guenther, 2002).

86 Isoprene, as the building block of the higher order isoprenoids, is the dominant
87 compound in emissions from many landscapes and has the single largest contribution to
88 total global vegetation BVOC emission, with an estimated global annual emission of about

89 400–600 Tg C (see Table 1 of Arneth et al., 2008). Even though there are more than 1000
90 monoterpene compounds identified in plants, only a few (less than 12) monoterpenes
91 comprise a large fraction of total monoterpene emissions into the atmosphere (Guenther,
92 2002). Compounds such as α -pinene, *t*- β -ocimene, β -pinene, limonene, sabinene, myrcene,
93 3-carene, camphene, β -phellandrene and terpinolene dominate monoterpene emissions
94 globally (Guenther et al., 2012). However, at regional scales other monoterpene compounds
95 may also be important (Geron et al., 2000; Jardine et al., 2015). Only a few (e.g., β -
96 caryophyllene) of about 3000 sesquiterpenes and none of the 2000 diterpenes are known to
97 be emitted into the atmosphere in considerable amounts (Guenther, 2002). However, there
98 are many compounds in the atmosphere that are still unknown or unexplored (Goldstein et
99 al., 2007, Park et al., 2013), suggesting that the characterization of sesquiterpene emissions
100 and other trace gases is still an open question.

101 Although models indicate that tropical rainforests are the main source of isoprenoid
102 emissions to the global atmosphere (Guenther et al., 2012), estimates of global annual
103 emissions of isoprenoid still have large uncertainties (Guenther et al., 2006). One approach
104 to constraining these estimates, specifically for isoprene, is the use of remotely sensed
105 concentrations of BVOC oxidation products in the atmosphere in order to make top-down
106 model estimates (Barkley et al., 2008, 2009, 2013; Stavrakou et al., 2009, 2015). This
107 approach has also suggested seasonal patterns in the emissions of this organic compound
108 (Barkley et al., 2009). In addition, seasonal variations of isoprene emissions in the
109 Amazonian rainforest are suggested based on comparison of some studies with intensive
110 campaigns *in situ* (Table 1). This seasonality may be driven by light and temperature
111 seasonal variation and leaf phenology (Barkley et al., 2009), and seasonal changes in
112 insolation is probably the main driver of leaf phenology (Jones et al., 2014).

113 Therefore, the objective of this study was to quantify the seasonal variation of
114 mixing ratios and emissions of isoprene, total monoterpenes and total sesquiterpenes in a
115 primary rainforest in central Amazonia and to correlate them to seasonal variations of
116 environmental (temperature and light) and biological (leaf phenology) factors.

117

118 **2. Material and methods**

119 **2.1 Site description**

120 Isoprenoid vertical profiles were investigated at the triangular tower (TT34 tower -
121 2°35.37'S, 60°06.92'W) on a plateau of the Cuieiras Biological Reserve, a primary
122 rainforest reserve located approximately 60 km northwest of Manaus city, in the central
123 Amazonian Basin, in Amazonas, Brazil (Martin et al., 2010). The vegetation in this area is
124 considered mature *terra firme* rain forest (Pires and Prances, 1985), with a leaf area index
125 of 4.7 (Malhi et al., 2009). The diversity of tree species is above 200 species ha⁻¹ (Oliveira
126 et al., 2008). Annual precipitation is about 2500 mm (Fig. 1a), with December to May
127 being the wetter period. Although severe droughts impacted part of the Amazon basin in
128 2005 and in 2010, those droughts did not affect central Amazonia (Marengo et al., 2008,
129 2011). However, micrometeorological measurements from 1999 to 2012 showed that from
130 August to September the monthly cumulative precipitation can be less than 100 mm per
131 month (Fig. 1a), characterizing this period as dry season. Average air temperature ranges
132 between 24 °C (in April) and 27 °C (in September) (Fig. 1e). Soil moisture near the surface
133 is slightly reduced (10%) during the dry compared to the wet season (Cuartas et al., 2012).

134 The period of this study (from September 2, 2010 to January 27, 2011) represents
135 the second half of the dry season (September 2010 - October 2010), the dry-to-wet
136 transition season (November 2010) and the beginning of the wet season (December 2010 -
137 January 2011). The whole period of measurements includes the period of low precipitation
138 and when precipitation is increasing (Fig. 1b), and when photosynthetically active radiation
139 (PAR) (Fig. 1d) and air temperature (Fig. 1f) are at their peaks. As October 2010 had more
140 precipitation only at the end of the month, for this study October 2010 is also considered as
141 dry season. This is supported by the fact that the length and intensity of the dry season
142 varies from year to year (da Rocha et al., 2009).

143

144 **2.2. Isoprenoid measurements and data analysis**

145 Ambient mixing ratio measurements of isoprene, total monoterpenes and total
146 sesquiterpenes were carried out using a commercial high sensitivity proton-transfer reaction
147 mass spectrometer (PTR-MS, IONICON, Austria). The PTR-MS was operated in standard

148 conditions with a drift tube voltage of 600 V and drift tube pressure of 2.0 mbar (E/N, 136
149 Td). During each PTR-MS measurement cycle, the following mass-to-charge ratios (m/z)
150 were monitored: 21 ($\text{H}_3^{18}\text{O}^+$), 32 (O_2^+), 37 ($\text{H}_2\text{O}-\text{H}_3\text{O}^+$) with a dwell time of 20 ms each; 69
151 (isoprene- H^+), 137 (total monoterpenes- H^+) and 205 (total sesquiterpenes- H^+) with a dwell
152 time of 5 s each (Jardine et al., 2011, 2012; Lindinger et al., 1998). The isoprenoid vertical
153 profile was installed with six ambient air inlets at different tower heights (2, 11, 17, 24, 30
154 and 40 m). Air was sequentially sampled during 10 min at each of the six heights, resulting
155 in one complete profile every hour. Average mixing ratios were calculated for the daytime
156 period (10:00 – 16:00, LT) and for the nighttime period (22:00 – 04:00, LT). Calibration
157 slope (m, ppbv/normalized counts per second (PTR-MS signal)) for isoprene, total
158 monoterpenes, and total sesquiterpenes were obtained twice in the field using the dynamic
159 solution injection technique (Jardine et al., 2010). Solutions of isoprene, α -pinene, and β -
160 caryophyllene standards (> 95% purity, Merk) in 100 mL of cyclohexane were injected into
161 the mixing vial at 0.5, 1.0, 2.0, and 3.0 $\mu\text{L min}^{-1}$ (30 min each flow rate) with a constant
162 dilution flow of 1.0 slpm ultra high purity nitrogen passing through. The linearity of
163 calibrations was significant, being r^2 of 0.92-0.97 for isoprene, r^2 of 0.98-0.99 for α -pinene,
164 and r^2 of 0.90-0.98 for β -caryophyllene. Sample air isoprenoid mixing ratios were
165 calculated by multiplying the calibration slope by normalized counts per second (PTR-MS
166 signal) (average of two calibration slopes). Calibration slopes obtained on October 2010
167 were within 10 % relative to those from the calibration carried out in September 2010
168 (isoprene 7.2 %, α -pinene – 8.2%, and β -caryophyllene – 2.5%). For 4-7 days before each
169 isoprenoid profile measurement period, ultra high purity nitrogen was run into the inlet of
170 the PTR-MS for 2 h in order to obtain the background signals. The limit of detection for
171 isoprene was 0.14 ppbv, 0.15 ppbv for total monoterpenes and 0.1 ppbv for total
172 sesquiterpenes. More details about calibration and experimental design can be obtained in
173 Jardine et al. (2011) and Jardine et al. (2012), in which a subset of these data are already
174 described. While the previous study considered a subset of this data and time period
175 (Jardine et al., 2011, 2012), this study examines the whole dataset and focuses on
176 seasonality of mixing ratios and fluxes. Also, this is the first study in central Amazonia that
177 correlates long-term measurements of isoprenoids, light and temperature, and leaf
178 phenology.

179

180 **2.3 Isoprenoid gradient flux, and modeled flux estimates - Model of Emissions of**
 181 **Gases and Aerosols from Nature (MEGAN 2.1)**

182 Fluxes of isoprene, total monoterpenes and total sesquiterpenes - for dry, dry-to-wet
 183 transition and wet seasons - were estimated using the average daytime (10:00-14:00, LT)
 184 concentration vertical profile throughout the canopy and applying an inverse Lagrangian
 185 transport model (ILT) (Raupach, 1989; Nemitz et al., 2000; Karl et al., 2004; Karl et al.,
 186 2009). The source/sink distributions throughout the canopy were computed according to
 187 Eq. (1):

$$188 \vec{C} - C_{Ref} = \vec{D} \cdot \vec{S} \quad (1)$$

189 where \vec{C} is the concentration (g m^{-3}) vector for the 6 levels, C_{Ref} is the concentration (g m^{-3})
 190 at reference height (40 m), \vec{D} (m) is a dispersion matrix, and \vec{S} ($\text{mg m}^{-2} \text{h}^{-1} \text{layer}^{-1}$) is the
 191 resulting source/sink vector. \vec{D} is expressed as a function of Lagrangian timescale and
 192 profiles of the standard deviation of the vertical wind speed (σ_w), which was normalized to
 193 friction velocity (u^*). Integration over all source and sink terms (\vec{S}) yielded the canopy
 194 scale isoprenoid flux ($\text{mg m}^{-2} \text{h}^{-1}$). To parameterize \vec{D} , we use the Lagrangian timescale (TI)
 195 parameterized according to Raupach (1989) and the vertical profile of the standard
 196 deviation of the vertical wind speed scaled to measured friction velocity. The normalized
 197 turbulence profile was taken from turbulence measurements inside and above the canopy at
 198 this site recorded as part of AMAZE-08 (Amazonian Aerosol Characterization Experiment
 199 2008) (Karl et al., 2009). The friction velocity was averaged for each season using daytime
 200 data (10:00-14:00, LT) measured at a tower (K34 tower - $2^\circ 36' 32.67''$ S, $60^\circ 12' 33.48''$
 201 W) that was 2 km away from the tower where isoprenoid profiles were measured (TT34
 202 tower). The calculation of \vec{D} was based on the far- and near-field approach described by
 203 Raupach (1989). As some model inputs (i.e., σ_w / u^*) were obtained during the wet season
 204 at the TT34 tower in 2008 (Karl et al., 2009), changes in canopy structure between the two
 205 studies could potentially affect the results of this study. However, previous work carried out
 206 at the K34 tower showed that u^* along with other averaged turbulence data have quite
 207 similar daytime values in both wet and dry seasons (Ahlm et al., 2010; Araujo et al., 2002).

208 Once fluxes from the isoprenoid vertical profiles were obtained by the ILT, they
 209 were compared with the isoprenoid fluxes estimated by the Model of Emissions of Gases
 210 and Aerosols from Nature (MEGAN 2.1). Isoprenoid emissions estimated by MEGAN 2.1
 211 are based on a simple mechanistic model that takes into account the main processes driving
 212 variations in emissions (Guenther et al., 2012). As described by Guenther et al., (2012), the
 213 activity factor for isoprene, monoterpenes and sesquiterpenes (γ_i) considers the emission
 214 response to light (γ_P), temperature (γ_T), leaf age (γ_A), soil moisture (γ_{SM}), leaf area index
 215 (LAI) and CO₂ inhibition (γ_{CO_2}) according to Eq. (2):

$$216 \quad \gamma_i = C_{CE} LAI \gamma_P \gamma_T \gamma_A \gamma_{SM} \gamma_{CO_2} \quad (2)$$

217 where C_{CE} is the canopy environment coefficient. For the present study, the canopy
 218 environment model of Guenther et al. (2006) was used. It has a C_{CE} of 0.57. MEGAN 2.1
 219 was run with variation in light and temperature and LAI. Leaf age of the foliage was
 220 estimated by the model based on changes in LAI. Soil moisture and CO₂ inhibition activity
 221 factors were assigned a value $\gamma_{SM} = 1$ and $\gamma_{CO_2} = 1$, respectively, which assumes no
 222 variation in these parameters. More details about the model settings can be obtained in
 223 Guenther et al. (2012).

224 Photosynthetic photon flux density (PPFD) and air temperature for all model runs
 225 were obtained from the K34 tower measurement time series (Program of Large Scale
 226 Biosphere-Atmosphere – LBA). LAI inputs were obtained by satellite observations from
 227 NASA MODIS during August 2010 to January 2011. The level-4 LAI product is
 228 composited every 8 days at 1-km resolution on a sinusoidal grid (MODIS-NASA, 2015).

229

230 **2.4 Uncertainties associated with the ILT and BVOC emission modeling**

231 The main source of errors for applying the ILT is related to the parameterization of
 232 two combined effects: (1) vertical diffusion coefficient which is based on measured
 233 $\sigma(w)/u^*$ profiles, and (2) Lagrangian dispersion time scale (Tl). Moreover, some
 234 uncertainties may be due to systematic error sources with respect to (3) chemical losses,
 235 and (4) the number of source layers. The entire parameterization of combined effect (1) and
 236 (2) was tested using data from an earlier study (Karl et al., 2009, Karl et al., 2010), where a
 237 comparison with eddy covariance measurements was available. Taking the above
 238 conservative error assessment, the combined (effect 1 and 2) uncertainty is +/- 30%.

239 To account for chemistry (effect 3) we used a simple modification of the diffusion
240 coefficient based on Hamba (1993), relying on the fact that the chemical loss will mainly
241 influence the far field of the parameterization. Based on estimated OH and measured O₃
242 densities (Karl et al. 2009, Karl et al., 2010) calculated VOC fluxes were corrected
243 accordingly. Due to low OH and O₃ densities in the canopy (<5 x 10⁵ molecules cm⁻³ for
244 OH and <10 ppbv for O₃) the chemical lifetime for isoprene and monoterpenes is
245 considered large compared to the mixing timescale, leading to a chemistry correction on the
246 order of <5% for isoprene and monoterpenes. This systematic error is included, but relies
247 on an estimation of OH for isoprene. The overall uncertainty for isoprene is calculated as
248 0.3 – 4 % by varying in-canopy OH densities between 5 x 10⁵ and 5 x 10⁶ molecules cm⁻³.
249 It is noted that an in-canopy OH density of 5 x 10⁶ molecules cm⁻³ is extremely unrealistic
250 in such a dense canopy and only serves as a very conservative upper limit. Those
251 assumptions were also considered for sesquiterpene flux estimates. However, a sensitivity
252 test was carried out to show if the increasing ozone concentrations during the dry season
253 could effectively affect sesquiterpene lifetime and then sesquiterpene flux estimates. For
254 this test, sesquiterpene lifetime was changed in the ILT model using a range from 2 min to
255 8 hours (upper limit used for isoprene and monoterpene flux estimates). The lower limit (2
256 min) is based on the lifetime calculated for β -caryophyllene when it is exposed to 24-h
257 average of 7 x 10¹¹ molecules cm⁻³ of ozone (~30 ppb) (Atkinson and Arey, 2003). If all
258 sesquiterpenes that occur in this site have similar reactivity with ozone as β -caryophyllene,
259 the overall uncertainty for sesquiterpene flux estimates is calculated as up to 20% by
260 varying sesquiterpene lifetime from 8 h to 2 min. It is noted that when considering a
261 lifetime range from 8h to 10 min, the uncertainty for sesquiterpene flux estimates is
262 calculated as up to 4%. The 20 % of uncertainty may be important only during the dry
263 season, when ozone mixing ratios can eventually reach 30 ppbv above canopy (40 m)
264 around noontime.

265 We have also investigated the effect of (4) - the number of source layers. If the
266 number of selected source layers is too small, systematic errors of the calculated integrated
267 fluxes arise. We have investigated this effect and found that in the present case, six source
268 layers are sufficient to capture >90% of the flux. In the present setup, the ILT model does
269 not converge for more than nine layers and the numerical solution becomes unstable. If the

270 ILT model was initiated to only calculate two source layers, the integrated flux would be
271 underestimated significantly (e.g. by up 50%). With 6 source layers we estimate a
272 systematic error of <10% due to this effect. The combined effect of the systematic errors
273 (3) and (4) is estimated to be 5-6%.

274 Random errors of the ILT parameterization for effects (1) and (2) mostly relate to
275 precision. Systematic errors (3) and (4) mostly relate to accuracy of the parameterization.
276 While there could also be combined effects of random and small systematic errors, that are
277 difficult to assess, we chose an overall conservative error estimate that should reflect
278 precision and accuracy for effects (1) and (2), noting that the 30% should mostly relate to
279 precision. All the uncertainties are one standard error.

280 With respect to uncertainties in model estimates, one of the first quantitative
281 estimates of biogenic VOC emissions (Lamb et al., 1987) included an estimate of
282 uncertainty of 210% based on the propagation of uncertainties in emission factors, emission
283 algorithms, amount of biomass, and land use distributions. This “factor of three”
284 uncertainty has continued to be used as a rough assessment of the uncertainty of biogenic
285 VOC emission model estimates applied on regional scales. A more recent study (Hanna et
286 al., 2005) attempted a comprehensive assessment of each model component and concluded
287 that the 95% confidence range on the calculated uncertainty in isoprene emission was about
288 one order of magnitude while the calculated uncertainty for monoterpenes and other VOC
289 was only $\pm 20\%$. Guenther (2013) suggests that the Hanna et al. (2005) study assigns
290 isoprene a higher uncertainty only because more is known about isoprene, and so there are
291 more parameters, and that the lack of observations for quantifying the uncertainties
292 associated with individual model parameters limits the usefulness of this uncertainty
293 estimation approach and instead recommends evaluations that consider the results of model
294 comparisons with canopy scale observations. These studies indicate that models tend to
295 agree with observations within $\sim 30\%$ for canopy scale studies with site specific parameters
296 (Lamb et al., 1996) or for regional scale estimates with known land cover (Misztal et al.,
297 2014) and differ by as much as a factor of two or more for other regional scale studies
298 (Muller et al., 2008; Warneke et al., 2010).

299

300 **2.5 Canopy light penetration and leaf phenology**

301 The standard canopy environment model of MEGAN 2.1 was used to model light
302 penetration into the canopy (Guenther et al., 2006). Model inputs included the above-
303 canopy PAR measured (every 30 min) at 50 m on the K34 tower for the whole period of
304 isoprenoid measurements as well as the estimated surface area density of the canopy (m^2
305 m^{-3}), with measurements carried out in March 2004 using a Light Detection and Ranging
306 sensor (LIDAR) in a transect on the same plateau area of this study (Parker and Fitzjarrald,
307 2004).

308 The light penetration was modeled for five canopy layers distributed from the
309 canopy top to the ground surface. The thickness of each of the five layers was determined
310 based on the canopy surface area density estimated for every 50 cm from the ground
311 surface to the top canopy (Parker and Fitzjarrald, 2004). The layers were distributed
312 according to a Gaussian curve fit to the canopy surface area densities (from 0.5 m to 48 m).
313 Light absorption was calculated as the difference in the model estimate of downward light
314 at the top and bottom canopy levels. This light absorption corresponded to light that passed
315 through the canopy vertically. Reflectance and scattering were not considered.

316 Leaf phenology was estimated based on the observation of leaf flushing events of
317 the upper crown surfaces of 63 living trees around the K34 tower (~ 2 km far of TT34
318 tower). For this approach, it is assumed that the leaf phenology of the upper crown surfaces
319 of trees around both towers is similar. For the monitoring, a system of data acquisition and
320 storage, based on a Stardot (model Netcam XL 3MP) camera with a 1024 x 768 resolution
321 CMOS sensor, was installed at K34 tower, at 15-20 m above the canopy. The camera
322 viewing angle was south azimuth, perpendicular to the solar transit, centered on 32° of
323 depression and pointing out to an area of plateau. Images were logged every 15 s to a
324 passively cooled FitPC2i with heat-tolerant SSD drive. The whole system of data
325 acquisition automatically rebooted after power outages. The images obtained by the camera
326 covered approximately 66° horizontally and 57° vertically, fitting the forest canopy without
327 including any area of sky in the image. The most distant trees in the image were located
328 150 m from the camera. The framework was fixed by monitoring the same 63 treetops over
329 four months of observation (October 2010 – January 2011). The analysis of images was

330 based on the number of treetops that showed leaf flushing within one month. For this, one
331 image was selected at every six days, and then grouped for each month of this study.

332

333 **2.6 Satellite-derived isoprene emission estimates**

334 Top-down isoprene emission estimates over the 0.5 degree region around TT34
335 tower were obtained by using a grid-based source inversion scheme (Stavrakou et al., 2009)
336 constrained by formaldehyde (HCHO) columns. HCHO is an intermediate product of the
337 isoprene degradation process (e.g. Stavrakou et al., 2014). It is measured by UV-visible
338 sensors, such as on the Global Ozone Monitoring Experiment (GOME-2)/MetOp satellite
339 launched in 2006. The source inversion was performed using the global chemistry-transport
340 model IMAGESv2 (Intermediate Model of Annual and Global Evolution of Species) run at
341 a resolution of $2^\circ \times 2.5^\circ$ and 40 vertical levels from the surface to the lower stratosphere
342 (Stavrakou et al., 2014, 2015). The priori isoprene emission inventory is taken from
343 MEGAN-MOHYCAN-v2 (Stavrakou et al., 2014,
344 <http://tropo.aeronomie.be/models/isoprene.htm>), and includes updates regarding isoprene
345 emission rates from Asian tropical forests. IMAGESv2 uses HCHO columns retrieved from
346 GOME-2 sensor as top-down constraints and estimates the posterior biogenic isoprene
347 emission on the global scale. Note that given the early morning (9:30) overpass time of the
348 GOME-2 measurement, and the mostly delayed production of formaldehyde from isoprene
349 oxidation, the top-down emission estimate is dependent on the ability of MEGAN to
350 simulate the diurnal shape of isoprene emission and on the parameterization of chemical
351 and physical processes affecting isoprene and its degradation products in IMAGESv2. For
352 this study, we use daily (24 hours) mean satellite-derived isoprene emissions derived from
353 January 2010 to January 2011. More details can be found in Stavrakou et al. (2009, 2014,
354 2015) and Bauwens et al. (2013).

355

356 3. Results and Discussion

357 3.1 Diurnal variation of isoprenoid mixing ratios

358 Vertical profiles of isoprenoids were analyzed for daytime and nighttime for all the
359 seasons considered in this study. Isoprene (Fig. 2 a, b, c) and total monoterpenes (Fig. 2 d,
360 e, f) had higher mixing ratios during daytime (10:00-16:00, LT) than during nighttime
361 (22:00-04:00, LT) for all seasons, supporting the findings that emissions of isoprene (Alves
362 et al., 2014; Harley et al., 2004) and monoterpenes (Bracho-Nunez et al., 2013; Kuhn et al.,
363 2002, 2004a; Jardine et al., 2015) from Amazonian plant species, at least at this site, are
364 primarily light-dependent and stimulated by increasing temperature.

365 During daytime, isoprene had a maximum mixing ratio within the canopy. By
366 comparison, at nighttime maximum values occurred above the canopy, and the vertical
367 profiles were similar to those of nighttime air temperature (Fig. 2 j, k, l). As isoprene is not
368 emitted at night, this maximum nighttime abundance of isoprene above the canopy may be
369 due to the daytime residual layer concentrations. In addition, isoprene lifetime increases
370 during nighttime owing to the decrease of OH (hydroxyl radical) concentrations in the dark
371 (Goldan et al., 1995) in light of the low concentrations of nitrogen oxides (NO_x) in
372 Amazonia (≤ 3 ppb above the canopy during nighttime in the dry-to-wet transition season)
373 (Andreae et al., 2002). Similar results found at another site in central Amazonia suggested
374 that low isoprene concentrations near the ground after sunset could be due to deposition
375 onto and consumption by surfaces (Yáñez-Serrano et al., 2015). Isoprene up-take in the soil
376 has been suggested previously in central Amazonia (Silva, 2010), possibly because of
377 isoprene microbial consumption (Cleveland and Yavitt, 1997; Gray et al., 2014). As with
378 isoprene, higher mixing ratios of total monoterpenes were observed during daytime,
379 indicating that they are light-dependent, which agrees with the evidence of recent
380 photosynthetic origin of monoterpenes (Jardine et al., 2015; Loreto et al., 1996).

381 The vertical profile of total sesquiterpene mixing ratios differed from that of
382 isoprene and total monoterpenes for all seasons. Total sesquiterpenes had higher mixing
383 ratios near the ground and at the sub-canopy level (17 m) than above the canopy (Fig. 2 g,
384 h, i) ($P < 0.05$). Daytime and nighttime vertical profiles had similar shape, but total
385 sesquiterpene mixing ratios were higher during the nighttime. Even though sesquiterpene
386 emissions for some plant species are both light- and temperature-dependent (Duhl et al.,

2008), results reported here indicate that sesquiterpene emissions are not strongly light-dependent in this site, suggesting that their daily variation is driven primarily by temperature. Since some studies have shown that sesquiterpenes are found in the essential oil stored in Amazonian forest trees (e.g. Lima et al., 2005), emissions from these storage structures would not be expected to be light-dependent. In contrast, the monoterpenes, while also present in Amazonian tree essential oil (e.g. Fidelis et al., 2012; Lima et al., 2005), appear to be dominated by emissions that occur with no storage (e.g. Loreto et al., 1996; Jardine et al., 2015), similar to isoprene emission processes. Another reason for the higher total sesquiterpene mixing ratios at nighttime might be because of the reduction of oxidative reactions owing to the decrease of OH concentrations in the dark (Goldan et al., 1995) and low concentrations of nitrogen oxides (NO_x) (Andreae et al., 2002), ozone, and nitrate (NO_3) in Amazonia (Martin et al., 2010). In addition, ozonolysis of sesquiterpenes during daytime can reduce ambient sesquiterpene concentrations, as previously reported for a subset of these data (Jardine et al., 2011). With daytime ozone mixing ratios up to 40 ppbv (40 m) during the dry season, sesquiterpene lifetime with respect to ozonolysis above the canopy (40 m) can be 2 min during the daytime and 5 min during the nighttime (Jardine et al., 2011). Additionally, sesquiterpene concentrations can build up near the surface, because during nighttime the storage in the forest dominates (80-90%) and is significantly larger than the turbulent flux (Karl et al., 2004).

406

407 **3.2 Seasonal variation on isoprenoid mixing ratios and emissions**

408 Vertical profiles of isoprene had higher mean mixing ratios in the dry season, followed by the dry-to-wet transition season and wet season (top panel of Fig. 3 a). The reduction of isoprene mixing ratios from the dry season to dry-to-wet transition season was up to 20% and from dry season to wet season was up to 65%. During the dry season, the higher mixing ratios and emissions of isoprene have been attributed to the higher insolation and higher temperatures compared to the wet season and, for this reason, higher isoprene concentrations at the top of the canopy are expected. Nevertheless, in contrast to the observations of Yañez-Serrano et al. (2015), who reported maximum daytime mixing ratios of isoprene at the top of the canopy for both dry and wet seasons, this study showed the

417 highest isoprene mixing ratios inside the canopy (11 m) during the dry season, with this
418 maximum moving to the upper canopy during the dry-to-wet transition season (24 m).

419 Isoprene emissions inferred from concentration vertical profiles were estimated to
420 be highest in the sub-canopy (16 m) during the dry season and in the upper canopy (28 m)
421 during the dry-to-wet transition season and the wet season (Fig. 4 a). Even though there
422 were differences in which layer was the highest emitter of isoprene within the canopy,
423 mean isoprene emissions into the atmosphere were about the same for the dry season and
424 the dry-to-wet transition season ($1.37 \pm 0.7 \text{ mg m}^{-2} \text{ h}^{-1}$ and $1.41 \pm 0.1 \text{ mg m}^{-2} \text{ h}^{-1}$,
425 respectively). Both of these seasons had higher isoprene emissions than during the wet
426 season ($0.52 \pm 0.1 \text{ mg m}^{-2} \text{ h}^{-1}$) (Fig. 4 b).

427 The maximum absorption of PPFD by canopy, calculated based on PPFD
428 penetration profile modeled by the standard MEGAN 2.1 canopy environment model,
429 occurred right above the maximum of estimated surface area density of the canopy, with
430 the absorption of PPFD being higher during the dry season, followed by the wet season and
431 the dry-to-wet transition season (Fig. 3 b). This maximum PPFD absorption at the upper
432 canopy agreed with the maximum of isoprene mixing ratios (top panel of Fig. 3 a) and
433 emissions (Fig. 4 a) during the dry-to-wet transition season. It differed, however, when
434 compared to peaks of isoprene mixing ratios and emissions during the dry season and the
435 wet season.

436 One reason for this difference could be the isoprene oxidation in the atmosphere and
437 within plant, especially at the top of the canopy. During the dry season the ratio of methyl
438 vinyl ketone + methacrolein + hydroperoxides (MVK+MAC+ISOPOOH) (Liu et al., 2013)
439 to isoprene was higher compared to the dry-to-wet transition and the wet season (data not
440 shown). This higher ratio may indicate an increased oxidative capacity of the atmosphere
441 during the dry season. Moreover, a small source of MVK+MAC+ISOPOOH was observed
442 at the top of the canopy (Jardine et al., 2012). Under conditions of high abiotic stress, as
443 can occur in the dry season, elevated isoprene oxidation rates in plants can be observed and
444 isoprene oxidation products might be directly emitted by plants (Jardine et al., 2012).

445 Another important factor might be leaf phenology and/or leaf demography.
446 Different tree species have different isoprene emissions rates, and these rates depend upon

447 the leaf ontogenetic stage. Isoprene emitters can flush at different canopy levels seasonally,
448 and changes in within-canopy isoprene vertical profiles would be expected as a result.
449 Moreover, as more leaf flushing was observed at the upper canopy during the wet-to-dry
450 transition and early dry season, this caused leaves in the age group of 3-8 months to reach
451 the highest abundance in late dry season and early wet season (Nelson *et al.*, 2014). The
452 period with the high abundance of leaves in this age group is coincident with the period
453 when gross ecosystem productivity and landscape-scale photosynthetic capacity is most
454 efficient (Restrepo-Coupe *et al.*, 2013). Here, results show maximum isoprene emission at
455 the upper canopy during the dry-to-wet transition season (Fig. 4 a), which is coincident
456 with the period of high abundance of healthy efficient leaves at the canopy top (Nelson *et*
457 *al.*, 2014) and also coincident with the maximum isoprene emission shown in young mature
458 leaves in the dry-to-wet transition season (Alves *et al.*, 2014). Similarly, higher isoprene
459 emissions during the late dry season have also been related to the increase of active
460 biomass in southern Amazonia (Kesselmeier *et al.*, 2002; Kuhn *et al.*, 2004a, 2004b).

461 Although the isoprene mixing ratios reported here are within the range of previously
462 reported values in central Amazonia for the dry season and the dry-to-wet transition season
463 (Greenberg and Zimmerman, 1984; Rasmussen and Khalil, 1988; Zimmerman *et al.*, 1988)
464 and for the wet season (Yáñez-Serrano *et al.*, 2015), these results are the lowest observed
465 fluxes of isoprene to atmosphere reported for the Amazonia. However, this could be due to
466 features associated with the site of this study, such as the relatively open canopy caused by
467 the proximity to a dirt road and perhaps a relatively low fraction of isoprene emitting
468 species. Isoprene fluxes measured previously at the same tower site during the wet season
469 were similar (Karl *et al.*, 2009).

470 Total monoterpenes also showed a strong seasonal variation with maximum mixing
471 ratios during the dry-to-wet season, followed by the dry season and the wet season (middle
472 panel of Fig. 3 a). Taking mixing ratios of the dry-to-wet transition season as a reference,
473 total monoterpene mixing ratios showed an increase of up to 20% from the dry season to
474 the dry-to-wet transition season, and a decrease of up to 50% from the dry-to-wet transition
475 season to the wet season. Although total monoterpene mixing ratios were somewhat higher
476 in the dry-to-wet transition season than during the dry season, total monoterpene fluxes
477 inferred by the vertical profiles were slightly higher during the dry season (1.47 ± 0.06 mg

478 $\text{m}^{-2} \text{h}^{-1}$) compared to the dry-to-wet season ($1.29 \pm 0.2 \text{ mg m}^{-2} \text{ h}^{-1}$) (Fig. 4 e), indicating that
479 the production is higher in the dry season and losses are also higher, leading to lower
480 mixing ratios. In comparison, emissions from these two seasons were considerably higher
481 than during the wet season ($0.36 \pm 0.05 \text{ mg m}^{-2} \text{ h}^{-1}$) (Fig. 4 e). This again indicates that
482 higher insolation and air temperature during the dry season and dry-to-wet transition season
483 compared to the wet season increased the atmospheric concentrations of monoterpenes and,
484 considering the enhanced ozone mixing ratios during the dry season, this may influence the
485 seasonal pattern in monoterpene ozonolysis loss rates (Jardine et al., 2015). These results
486 agree with branch level measurements that showed higher monoterpene emissions during
487 the dry-to-wet transition season compared to the wet-to-dry transition season (Kuhn et al.,
488 2004a). However, results reported here differ from those presented for the southern
489 Amazonia, where monoterpene mixing ratios were higher during the wet season than
490 during the dry season (Kesselmeier et al., 2002). Although only a few studies have been
491 carried out with the objective of investigating monoterpene seasonal variations, factors
492 other than light and temperature might influence monoterpene emissions from vegetation,
493 including the oxidative capacity of the atmosphere and leaf phenology (Kesselmeier et al.,
494 2002; Kuhn et al., 2004a).

495 Total monoterpene mixing ratios and fluxes, during the dry season and the dry-to-
496 wet transition season, were similar to values reported for other sites in central Amazonia
497 (Karl et al., 2007; Yáñez-Serrano et al., 2015). However, the monoterpene comparison of
498 reported studies is a difficult endeavor given that some techniques measured total
499 monoterpenes and others measured some specific monoterpene compounds, and also
500 because monoterpene fragmentation during measurements (PTR-MS) could affect the
501 absolute values of these compounds. Therefore, further efforts are needed in order to
502 characterize the seasonal abundance and the seasonal species-specific composition of
503 monoterpenes in the Amazonia.

504 Average vertical profiles of total sesquiterpene mixing ratios were higher in the dry-
505 to-wet transition season, followed by the dry season and the wet season (bottom panel of
506 Fig. 3a). Taking mixing ratios of the dry-to-wet transition season as a reference, total
507 sesquiterpene mixing ratios increased up to 30% from the dry season to the dry-to-wet
508 transition season and decreased by up to 55% from the dry-to-wet transition season to the

509 wet season. During the dry season and the dry-to-wet transition season, the maximum total
510 sesquiterpene mixing ratios were observed near the ground. During the wet season, the
511 maximum mixing ratio was at 17 m (sub-canopy). According to Jardine et al. (2011),
512 during the daytime many sesquiterpenes (46%–61% by mass) are rapidly oxidized by ozone
513 as they undergo within-canopy ozonolysis and contribute to the scarcity of total
514 sesquiterpenes above and near the top of the canopy. Considering that higher insolation and
515 also higher ozone concentrations were observed during the dry season (ozone daily average
516 of ~ 23 ppbv and ~ 10 ppbv at 40 m in the dry and wet seasons, respectively), an important
517 fraction of the sesquiterpenes emitted by vegetation could be rapidly oxidized by ozone,
518 leading to significantly lower mixing ratios of total sesquiterpene during the dry season
519 (Jardine et al., 2011), which creates a need to account for sesquiterpene oxidation within
520 the canopy when calculating emission rates.

521 Another potential reason for higher mixing ratios of total sesquiterpenes near the
522 ground is that emission could come from surface sources including litter, roots and soil
523 microbes and fungi. Silva (2010) presented surface BVOC emissions at this site, and the
524 results suggested that the litter decomposition could be an important source of
525 sesquiterpenes to the atmosphere. Litter production is higher during the dry than during the
526 wet season (Luizão et al., 1989), which could lead to higher amounts of litter at the end of
527 the dry season. Rain starting to increase in the dry-to-wet transition could contribute to
528 more decomposition of the litter storage, which can potentially increase sesquiterpene
529 emissions during the processes of decomposition of dead organic matter. Although the
530 ecological functional role of these sesquiterpenes is not known, abiotic emissions from the
531 litter have a specific signature that can be similar to the concentration profile in the green
532 leaf content (Austin et al., 2014) and in sufficient concentration BVOCs can have the
533 capacity of attracting and repelling soil organisms to a specific location (Austin et al.,
534 2014). Therefore, higher sesquiterpene emissions from the litter could be a signal to the
535 fauna related to the decomposition process and represent an important step of the
536 biogeochemical cycling.

537 In contrast to the mixing ratios, the source-sink distribution analysis made from the
538 vertical profiles of total sesquiterpenes indicated that the main source of these compounds
539 is the canopy (24 m) (Fig. 4 g), and the integration of sources and sinks showed that the

540 highest total sesquiterpene emission rates going into the atmosphere was during the dry-to-
541 wet transition season ($0.77 \pm 0.1 \text{ mg m}^{-2} \text{ h}^{-1}$), followed by the dry season ($0.38 \pm 0.2 \text{ mg m}^{-2}$
542 h^{-1}), and the wet season ($0.34 \pm 0.2 \text{ mg m}^{-2} \text{ h}^{-1}$) (Fig. 4 h). However, although Nemitz et al.
543 (2000) have suggested that limitations on the σ_w/u^* parameterization close to the ground do
544 not affect the net flux above the canopy, here we strongly suggest future studies focus on
545 better characterizing the turbulence and oxidation processes at this site, in order to verify
546 the source-sink distribution of sesquiterpenes within the canopy and the emissions from the
547 canopy to atmosphere. This should include speciated sesquiterpene measurements in order
548 to account for their specific reactivity with ozone and other oxidants.

549 Relative emissions can be calculated as emissions normalized to standard conditions
550 of above-canopy PAR of $1500 \mu\text{mol m}^{-2} \text{ s}^{-1}$ and temperature of $30 \text{ }^\circ\text{C}$. Based only on light,
551 temperature and LAI variation, relative emissions estimated by MEGAN 2.1 were
552 maximum during the dry season for isoprene, α -pinene, and β -caryophyllene (Fig. 4 c, f, i),
553 when the highest light and temperature were observed. This prediction differs from the ILT
554 flux estimates (Fig. 4 b, e, h), which showed similar emissions between the dry and the dry-
555 to-wet season for isoprene and total monoterpenes and maximum emission during the dry-
556 to-wet season for total sesquiterpenes. The overall uncertainties related to ILT flux was
557 calculated as $\pm 36\%$ and MEGAN estimates are considered to be in agreement with
558 observations when they are within $\sim 30\%$. However, more observation studies are needed in
559 order to evaluate the degree of observation-modeling agreement and to improve model
560 approaches, especially for total monoterpenes and total sesquiterpenes, which could present
561 larger uncertainties due to the lack of information about atmospheric concentrations and
562 reactivity of monoterpene and sesquiterpene chemical species in Amazonia.

563 To compare the seasonal variation of isoprenoid emissions with changes in
564 environmental (light and temperature) and biological (LAI) factors in more detail, monthly
565 fluxes of isoprenoids were compared to PAR at 51 m, air temperature at 51 m, and LAI
566 (satellite observations - MODIS) (Fig. 5). The highest fluxes of isoprene and total
567 monoterpene were observed when PAR was at its highest (October 2010) (Fig. 5 b, c), and
568 when there is high abundance of healthy efficient leaves (Nelson et al., 2014). The
569 similarity in the behavior of isoprene and monoterpene emissions is supported by the
570 evidence of the photosynthetic origin of monoterpenes (Jardine et al., 2015; Loreto et al.,

1996). Interestingly, in September 2010 total monoterpene emissions were higher than isoprene emissions. This could be related to the higher source of monoterpenes in the upper canopy compared to isoprene during this month. When there are more young leaves at the upper canopy during the first half of the dry season (Nelson et al., 2014), high emissions of monoterpenes can be expected. Total sesquiterpene fluxes tracked neither PAR nor air temperature, having the highest emission when PAR and air temperature were decreasing (November 2010) (Fig. 5 d).

Predictions from MEGAN 2.1 again differed from measured emissions (Fig. 5 b, c, d), showing a reduction in emissions from September 2010 to January 2011. Major quantitative differences between ILT and MEGAN estimates can be shown for isoprene in September, when ILT estimates represented only 4 % of the MEGAN estimates; for total monoterpenes in December, when ILT estimates accounted for 14 % of the MEGAN estimates; and for total sesquiterpenes in November, when ILT estimates were 232% of the MEGAN estimates". These differences may be related to local effects, especially leaf phenology and changes in the atmospheric oxidative capacity over the seasons. In order to evaluate the potential effect of leaf phenology on emissions, leaf flushing, PAR, isoprene and total monoterpenes at canopy scale were compared in Fig. 6. They closely tracked each other during the 4 months of measurements. For the period of this study, the analysis of canopy images for every six days from October 2010 to January 2011 showed a decrease in leaf flushing from the end of the dry season to the wet season, which was similar to the decrease of isoprene and total monoterpene emissions and PAR. Results from 28 months (October 2010-January 2013) of canopy imaging have shown that the highest number of treetops with leaf flushing occurred during the wet-to-dry transition season (June-July), accounting for 35-50 % of treetops with leaf flushing, followed by a subsequent decrease until the end of the wet season (Tavares, 2013) (Fig. 6). Correspondingly, the results of the present study suggest that lowest emissions might be expected in the June-July time period. These results agree with those presented by Barkley et al. (2009) using remote sensing, suggesting that seasonal changes in isoprene emissions may be strongly affected by leaf phenology in the Amazonia.

In order to verify if the seasonal trend of the isoprene emissions observed in this study can also be observed in a 0.5° grid cell around TT34 tower, isoprene emissions

602 estimated based on tower vertical profile concentrations are compared with estimates
603 constrained by satellite measurements of HCHO in Fig. 7. The top-down estimates have a
604 seasonal cycle that is similar to the bottom-up approach. Compared to the dry season,
605 fluxes decrease by 40% during the wet and the wet-to-dry transition season from April to
606 July (Stavrakou et al., 2015), in qualitative agreement with the conclusions drawn in
607 Barkley et al. (2009). The inferred dry season isoprene flux is about twice that of the wet-
608 to-dry season. It peaks in September and gradually drops from October to January (Fig. 7),
609 as a result of decreasing temperature and solar radiation, affecting the oxidation of isoprene
610 leading to HCHO formation. The ground-based estimates exhibit a much stronger month-
611 to-month variation, with flux estimates of 5 times higher in October compared to
612 September and December. The small increase of the flux between December and January is
613 not observed by the satellite observations. Despite these differences, partly due to reduced
614 representativeness when comparing local measurements with flux estimates from a 0.5°
615 grid cell, this comparison shows that both large (satellite) and small (ground-based) scales
616 agree that there are enhanced isoprene emissions during the dry season followed by a
617 reduction towards the wet season.

618 The results reported here are associated with a small footprint area. This together
619 with the huge biodiversity of tropical rainforests makes it impossible to generalize these
620 results to the regional scale. Moreover, although some previous reports have suggested
621 significant seasonal variations of BVOCs based on *in situ* measurements in different sub-
622 regions of Amazonia, when those investigations (summarized in Table 1) and this study
623 were compared, high variability is apparent among values of mixing ratios and fluxes. This
624 variability could be due to: (1) different methodologies, (2) sampling in different seasons,
625 (3) sampling in different regions (e.g., south, north, west, eastern Amazonia), (4) sampling
626 in different ecotones of the same region, (5) different statistical analyses, and (6) perhaps
627 due to small data sets that are not statistically significant to characterize emissions of a
628 specific site.

629

630 **3.3 Comparison with model predictions of seasonal isoprenoid emissions in Amazonia**

631 Although the canopy scale isoprenoid emission measurements presented here
632 differed from those modeled by MEGAN 2.1 (Figs. 4 and 5), which assume that variations

633 are driven primarily by light, temperature and leaf area, in terms of seasonal variation,
634 MEGAN 2.1 estimates of isoprene emission agreed fairly well with the satellite-derived
635 isoprene emission, which suggests that other factors at this site could influence isoprene
636 emissions locally. As already mentioned, leaf phenology may cause important effects on
637 local emissions. As MEGAN 2.1 was driven with local variations in PAR and air
638 temperature, and with regional variations of LAI (satellite observations at 1-kilometer
639 resolution), this regional variation in LAI may not represent the local effect of LAI
640 variation on local emissions, since vegetation in Amazonia is phenologically distinct due to
641 the huge biodiversity of this ecosystem (Silva et al., 2013). Furthermore, as the canopy
642 structure might vary seasonally due to leaf phenology/demography, the pattern of light
643 penetration/absorption and then leaf temperature may change as well; thus, this, together
644 with the differences in emissions among species and among leaf ontogenetic stages, could
645 have an important impact on seasonal changes of local emissions.

646 Besides the effects of light, temperature and leaf phenology/demography, some
647 efforts have been made to include effects of CO₂ variation (Arneeth et al., 2007; Guenther et
648 al., 2012) as well as the link between photosynthesis and emission (Grote et al., 2014;
649 Morfopoulos et al., 2013, 2014; Unger et al., 2013) into isoprene emission models at
650 regional and global scales. However, the current regional and global BVOC emission
651 models predict much smaller seasonal variations (Guenther et al., 2006, 2012; Muller et al.,
652 2008; Unger et al., 2013) compared to the measurements in Amazonia (Table 1).
653 Furthermore, satellite observations indicate that the current understanding of the processes
654 controlling seasonal variations is insufficient, and models do not simulate the unexpected
655 shutdown of isoprene emission in the Amazonia during the wet-to-dry transition season
656 (Barkley et al., 2009).

657 Many recently published studies have used the MEGAN model and the majority
658 have focused on improving our understanding of isoprene emissions. Although other
659 models have been developed on the basis of known biochemical processes (Grote et al.,
660 2014; Morfopoulos et al., 2014; Unger et al., 2013), the general framework and processes
661 simulated are similar. The biochemical basis of isoprene production and release must be
662 further understood to develop mechanistic explanations for variation in isoprene emission

663 (Monson et al., 2012), which may reduce uncertainties associated with the responses to
664 environmental factors.

665 Seasonal variation of isoprene emissions might be explained by the change in
666 energy supply from photosynthesis throughout the seasons (e.g. Grote et al., 2014). This is
667 supported by the generally strong correlation between isoprene emission and gross
668 photosynthetic capacity reported for Amazonian tree species (Kuhn et al., 2004b), and by
669 the fact that higher demography of healthy efficient leaves (Nelson et al., 2014) coincides
670 with the period of most efficient landscape-scale photosynthesis and photosynthetic
671 capacity (Restrepo-Coupe et al., 2013). However, more measurements are needed to
672 examine this relationship which should follow PAR variation. Additionally, since canopy
673 structure may explain some variation in biomass growth over tropical landscapes due to
674 differences in the pattern of light penetration and absorption by the canopies (Stark et al.,
675 2012), measurements of canopy structure may also help to explain some of the differences
676 in isoprenoid emissions among the Amazonian sub-regions.

677 Therefore, at least for the Amazonian rainforest, models currently do not fully
678 capture seasonal variations in isoprenoid emissions, especially for monoterpenes and
679 sesquiterpenes, which are less investigated compared to isoprene. The scarcity of
680 measurements in Amazonia prevents the development and evaluation of accurate model
681 approaches. Thus, this study strongly encourages future *in situ* measurements in Amazonia,
682 including at leaf level, in order to verify changes driven by seasonal variations in leaf area,
683 leaf age, phenology and emission response to soil moisture, and the short-term and long-
684 term temperature and light environment.

685

686 **4. Summary and conclusions**

687 In this study, we present the first *in situ* measurements that show a seasonal trend in
688 isoprenoid emissions for a primary rainforest of central Amazonia. Isoprenoid emissions
689 peak at the end of the dry season and at the dry-to-wet transition season. Under conditions
690 of high insolation and high temperatures joined together with the high demography of
691 photosynthetically efficient leaves (Caldararu et al., 2012; Myneni et al., 2007; Nelson et
692 al., 2014; Samanta et al., 2012), isoprenoid metabolic pathways may experience more
693 favorable conditions for synthesizing these compounds in the dry season and the dry-to-wet

694 transition season. This is especially for the case of isoprene and monoterpenes, which are
695 light- and temperature-dependent and are affected by the recent production of
696 photosynthetic substrates.

697 Although some studies have suggested that there are no seasonal variations in
698 canopy structure and greenness in Amazonia (e.g. Morton et al., 2014), results reported
699 here present a seasonal variation of leaf flushing and suggest maximum leaf demography in
700 the late dry season, which generally agrees with the assumption that a greenup during the
701 dry season in Amazonia may drive increasing isoprene emissions as suggested by satellite
702 retrievals (Barkley et al., 2009). Moreover, this study also suggests that seasonal changes in
703 the atmospheric oxidative capacity could have an important impact on the seasonality of at
704 least some isoprenoid concentrations and above canopy emissions, especially for
705 sesquiterpenes. Their quantification is challenged by rapid atmospheric chemical reactions
706 catalyzed by high insolation and higher ozone concentrations in the dry season.

707 MEGAN 2.1 estimates did not fully capture the behavior observed with the
708 isoprenoid emissions based on in-situ PTR-MS measurements (inverse Lagrangian
709 transport model). Model emissions of isoprene and total monoterpenes were overestimated,
710 especially during September 2010 (dry season) and December 2010 (wet season),
711 respectively. Total sesquiterpenes were underestimated during November 2010 (dry-to-wet
712 transition season). This difference between MEGAN 2.1 flux estimates and fluxes
713 estimated by the PTR-MS vertical mixing ratio profiles could be due to experimental errors
714 or the influence of very local effects on the seasonal emissions measured in this site,
715 because satellite-derived isoprene emissions agree fairly well with MEGAN 2.1 emission
716 estimates and the ground observations do not agree with the satellite data or the model,
717 principally in September. Perhaps the isoprene pattern observed at the site is due to a very
718 local effect of leaf flushing by isoprene emitting species around this tower, but this is not
719 seen on the regional scale where there are different species distributions.

720 Generally, current models assume that seasonal variation of BVOC emissions in the
721 Amazonian rainforest are primarily based on light and temperature variations. These model
722 simulations capture only a part of the actual variation and have uncertainties associated
723 with the insufficient understanding of mechanistic processes involved in the seasonality of
724 these compounds. Nevertheless, because the number of measurements and sites is limited in

725 Amazonia, there is a scarcity of information, which hinders further model improvements. In
726 summary, our results demonstrate strong seasonality and suggest that important processes
727 are taking place during the transition seasons. Also, results reveal the need for long-term
728 and continuous BVOC observations from leaf level to ecosystem level, and also suggest
729 that standardized measurement procedures are required in order to compare the different
730 Amazonian sub-regions. This may advance understanding of the seasonality of BVOC
731 exchanges between forest and atmosphere, providing the information needed to improve
732 BVOC emission estimates for climate and air quality modelling studies.

733

734 **Acknowledgements**

735 This work was performed at the National Institute for Amazon Research and at the State
736 University of Amazonas with funding provided by the CNPq (fellowship provided to E.
737 Alves by the Brazilian government), and financial support for field work was provided by
738 the Philecology Foundation of Fort Worth, Texas, and the National Science Foundation
739 through the AMAZON-PIRE (Partnerships for International Research and Education)
740 award (0730305) and instrumentation support (CHE 0216226). We also thank Dr. Scott
741 Saleska for supporting this long field campaign. This research was also supported by the
742 Office of Biological and Environmental Research of the U.S. Department of Energy under
743 Contract No. DE-AC02-05CH11231 as part of their Terrestrial Ecosystem Science
744 Program. The authors would like to acknowledge the advice and support from the Large
745 Biosphere-Atmosphere (LBA) as a part of the Green Ocean Amazon (GoAmazon) 2014/5
746 project in Manaus, Brazil. T. Stavrakou was supported by the GlobEmission project (No
747 4000104001/11/I-NB) of the European Space Agency.

748 **References**

749 Ahlm, L., Nilsson, E. D., Krejci, R., Mårtensson, E. M., Vogt, M. and Artaxo, P.: A comparison of dry and
750 wet season aerosol number fluxes over the Amazon rain forest, *Atmos. Chem. Phys.*, 10(6), 3063–3079,
751 doi:10.5194/acp-10-3063-2010, 2010.

- 752 Alves, E. G., Harley, P., Gonçalves, J. F. D. C., Eduardo, C. and Jardine, K.: Effects of light and temperature
753 on isoprene emission at different leaf developmental stages of *Eschweilera coriacea* in central Amazon, *Acta*
754 *Amaz.*, 44(1), 9–18, doi: 10.1590/S0044-59672014000100002, 2014.
- 755 Andreae, M. O., Artaxo, P., Brandao, C., Carswell, F. E., Ciccioli, P., da Costa, A. L., Culf, A. D., Esteves, J.
756 L., Gash, J. H. C., Grace, J., Kabat, P., Lelieveld, J., Malhi, Y., Manzi, A. O., Meixner, F. X., Nobre, A. D.,
757 Nobre, C., Ruivo, M., Silva-Dias, M. A., Stefani, P., Valentini, R., von Jouanne, J. and Waterloo, M. J.:
758 Biogeochemical cycling of carbon, water, energy, trace gases, and aerosols in Amazonia: The LBA-
759 EUSTACH experiments, *J. Geophys. Res.*, 107(D20), doi: 8066 10.1029/2001jd000524, 2002.
- 760 Aquino, C. A. B.: Identificação de Compostos Orgânicos Voláteis (COVs) emitidos por Florestas na região
761 Amazônica [*in Portuguese*], Master thesis. Federal University of Mato Grosso, Cuiabá-MT, Brazil, 106 pp.,
762 2006.
- 763 Araujo, A. C., Nobre, A. D., Kruijt, B., Elbers, J. A., Dallarosa, R., Stefani, P., von Randow, C., Manzi, A.
764 O., Culf, A. D., Gash, J. H. C., Valentini, R., Kabat, P. and Araújo, A. C.: Comparative measurements of
765 carbon dioxide fluxes from two nearby towers in a central Amazonian rainforest: The Manaus LBA site, *J.*
766 *Geophys. Res.*, 107(D20), 8090, doi:8090 10.1029/2001jd000676, 2002.
- 767 Arneth, A., Monson, R. K., Schurgers, G., Niinemets, U. and Palmer, P. I.: Why are estimates of global
768 terrestrial isoprene emissions so similar (and why is this not so for monoterpenes)?, *Atmos. Chem. Phys.*,
769 8(16), 4605–4620, doi:10.5194/acp-8-4605-2008, 2008.
- 770 Arneth, A., Niinemets, U., Pressley, S., Back, J., Hari, P., Karl, T., Noe, S., Prentice, I. C., Serca, D., Hickler,
771 T., Wolf, A. and Smith, B.: Process-based estimates of terrestrial ecosystem isoprene emissions: incorporating
772 the effects of a direct CO₂-isoprene interaction, *Atmos. Chem. Phys.*, 7, 31–53, doi:10.5194/acp-7-31-2007,
773 2007.
- 774 Atkinson, R. and Arey, J.: Atmospheric Degradation of Volatile Organic Compounds, *Chem. Rev.*, 103(3),
775 4605–4638, doi:10.1021/cr0206420, 2003.
- 776 Austin, A. T., Vivanco, L., González-Arzac, A. and Pérez, L. I.: There's no place like home? An exploration
777 of the mechanisms behind plant litter-decomposer affinity in terrestrial ecosystems, *New Phytol.*, 204(2),
778 307–314, doi:10.1111/nph.12959, 2014.
- 779 Barkley, M. P., Palmer, P. I., Kuhn, U., Kesselmeier, J., Chance, K., Kurosu, T. P., Martin, R. V., Helmig, D.
780 and Guenther, A.: Net ecosystem fluxes of isoprene over tropical South America inferred from Global Ozone
781 Monitoring Experiment (GOME) observations of HCHO columns, *J. Geophys. Res.*, 113(D20), D20304,
782 doi:10.1029/2008JD009863, 2008.
- 783 Barkley, M. P., Palmer, P. I., De Smedt, I., Karl, T., Guenther, A. and Van Roozendaal, M.: Regulated large-
784 scale annual shutdown of Amazonian isoprene emissions?, *Geophys. Res. Lett.*, 36(4), L04803,
785 doi:10.1029/2008GL036843, 2009.

- 786 Barkley, M. P., Smedt, I. De, Van Roozendaal, M., Kurosu, T. P., Chance, K., Arneeth, A., Hagberg, D.,
787 Guenther, A., Paulot, F., Marais, E. and Mao, J.: Top-down isoprene emissions over tropical South America
788 inferred from SCIAMACHY and OMI formaldehyde columns, *J. Geophys. Res. Atmos.*, 118(12), 6849–
789 6868, doi:10.1002/jgrd.50552, 2013.
- 790 Bauwens, M., Stavrakou, T., Müller, J. F., De Smedt, I., Van Roosendaal, M.: Satellite-based isoprene
791 emission estimates (2007-2012) from the GlobEmission projet, ACCENT-Plus Symposium, Atmospheric
792 Composition Change: the European Network", Urbino, 17-20 September, 2013.
- 793 Bracho-Nunez, A., Knothe, N. M., Welter, S., Staudt, M., Costa, W. R., Liberato, M. A. R., Piedade, M. T. F.
794 and Kesselmeier, J.: Leaf level emissions of volatile organic compounds (VOC) from some Amazonian and
795 Mediterranean plants, *Biogeosciences*, 10(9), 5855–5873, doi:10.5194/bg-10-5855-2013, 2013.
- 796 Caldararu, S., Palmer, P. I. and Purves, D. W.: Inferring Amazon leaf demography from satellite observations
797 of leaf area index, *Biogeosciences*, 9(4), 1389–1404, doi:10.5194/bg-9-1389-2012, 2012.
- 798 Ciccioli, P., Brancaleoni, E., Frattoni, M., Kuhn, U., Kesselmeier, J., Dindorf, T., De Araujo, A. C., Nobre, A.
799 D., Stefani, P. and Velentini, R.: Fluxes of isoprenoid compounds over the tropical rainforest near Manaus
800 during the dry season and their implications in the ecosystem carbon budget and in the atmospheric chemistry
801 processes, Report Series in Aerosol Science (62A) Proceedings of Integrated Land Ecosystem Atmosphere
802 Processes Study (ILEAPS) International Open Science Conference, Helsinki, Finland, 29 September – 3
803 October, ISBN 952-5027-40-6, 2003.
- 804 Cleveland, C. C. and Yavitt, J. B.: Consumption of atmospheric isoprene in soil, *Geophys. Res. Lett.*, 24(19),
805 2379–2382, doi:10.1029/97GL02451, 1997.
- 806 Cuartas, L. A., Tomasella, J., Nobre, A. D., Nobre, C. A., Hodnett, M. G., Waterloo, M. J., Oliveira, S. M.
807 De, Randow, R. D. C. Von, Trancoso, R. and Ferreira, M.: Distributed hydrological modeling of a micro-
808 scale rainforest watershed in Amazonia: Model evaluation and advances in calibration using the new HAND
809 terrain model, *J. Hydrol.*, 462-463, 15–27, doi:10.1016/j.jhydrol.2011.12.047, 2012.
- 810 da Rocha, H. R., Manzi, A. O., Cabral, O. M., Miller, S. D., Goulden, M. L., Saleska, S. R., R-Coupe, N.,
811 Wofsy, S. C., Borma, L. S., Artaxo, P., Vourlitis, G., Nogueira, J. S., Cardoso, F. L., Nobre, A. D., Kruijt, B.,
812 Freitas, H. C., von Randow, C., Aguiar, R. G. and Maia, J. F.: Patterns of water and heat flux across a biome
813 gradient from tropical forest to savanna in Brazil, *J. Geophys. Res.*, 114, G00B12,
814 doi:10.1029/2007JG000640, 2009.
- 815 Davis, K. J., Lenschow, D. H. and Zimmerman, P. R.: Biogenic nonmethane hydrocarbon emissions
816 estimated from tethered balloon observations, *J. Geophys. Res.*, 99(D12), 25587, doi:10.1029/94JD02009,
817 1994.
- 818 Duhl, T. R., Helmig, D. and Guenther, A.: Sesquiterpene emissions from vegetation: a review,
819 *Biogeosciences*, 5(3), 761–777, doi:10.5194/bg-5-761-2008, 2008.

- 820 Fidelis, C. H. V., Augusto, F., Sampaio, P. T. B., Krainovic, P. M. and Barata, L. E. S.: Chemical
821 characterization of rosewood (*Aniba rosaeodora* Ducke) leaf essential oil by comprehensive two-
822 dimensional gas chromatography coupled with quadrupole mass spectrometry, *J. Essent. Oil Res.*, 24(3), 245–
823 251, doi:10.1080/10412905.2012.676770, 2012.
- 824 Geron, C., Rasmussen, R., R. Arnts, R. and Guenther, A.: A review and synthesis of monoterpene speciation
825 from forests in the United States, *Atmos. Environ.*, 34(11), 1761–1781, doi:10.1016/S1352-2310(99)00364-7,
826 2000.
- 827 Goldan, P. D., Kuster, W. C., Fehseneld, F. C. and Montzka, S. A.: Hydrocarbon measurements in the
828 southeastern United States: The Rural Oxidants in the Southern Environment (ROSE) Program 1990, *J.*
829 *Geophys. Res.*, 100, 25945, doi:10.1029/95JD02607,1995.
- 830 Goldstein, A. H. and Galbally, I. E.: Known and Unexplored Organic Constituents in the Earth’s Atmosphere,
831 *Environ. Sci. Technol.*, 41(5), 1514–1521, doi:10.1021/es072476p, 2007.
- 832 Gray, C. M., Monson, R. K. and Fierer, N.: Biotic and abiotic controls on biogenic volatile organic compound
833 fluxes from a subalpine forest floor, *J. Geophys. Res. Biogeosciences*, 119(4), 547–556,
834 doi:10.1002/2013JG002575, 2014.
- 835 Greenberg, J. P., Guenther, A. B., Petron, G., Wiedinmyer, C., Vega, O., Gatti, L. V, Tota, J. and Fisch, G.:
836 Biogenic VOC emissions from forested Amazonian landscapes, *Glob. Chang. Biol.*, 10(5), 651–662,
837 doi:10.1111/j.1529-8817.2003.00758.x, 2004.
- 838 Greenberg, J. P. and Zimmerman, P. R.: Nonmethane hydrocarbons in remote tropical, continental, and
839 marine atmospheres, *J. Geophys. Res.*, 89(D3), 4767, doi:10.1029/JD089iD03p04767, 1984.
- 840 Grote, R., Morfopoulos, C., Niinemets, Ü., Sun, Z., Keenan, T. F., Pacifico, F. and Butler, T.: A fully
841 integrated isoprenoid emissions model coupling emissions to photosynthetic characteristics., *Plant. Cell*
842 *Environ.*, 37(8), 1965–80, doi:10.1111/pce.12326, 2014.
- 843 Guenther, A. B., Jiang, X., Heald, C. L., Sakulyanontvittaya, T., Duhl, T., Emmons, L. K. and Wang, X.: The
844 Model of Emissions of Gases and Aerosols from Nature version 2.1 (MEGAN2.1): an extended and updated
845 framework for modeling biogenic emissions, *Geosci. Model Dev.*, 5(2), 1503–1560, doi:10.5194/gmdd-5-
846 1503-2012, 2012.
- 847 Guenther, A., Karl, T., Harley, P., Wiedinmyer, C., Palmer, P. I. and Geron, C.: Estimates of global terrestrial
848 isoprene emissions using MEGAN (Model of Emissions of Gases and Aerosols from Nature), *Atmos. Chem.*
849 *Phys.*, 6(1), 3181–3210, doi:10.5194/acpd-6-107-2006, 2006.
- 850 Guenther, A.: The contribution of reactive carbon emissions from vegetation to the carbon balance of
851 terrestrial ecosystems, *Chemosphere*, 49(8), 837–44, doi:10.1016/S0045-6535(02)00384-3, 2002.

- 852 Guenther, A. B.: Upscaling biogenic volatile compound emissions from leaves to landscapes, in *Biology,*
853 *controls and models of tree volatile organic compound emissions*, edited by Ü. Niinemets and R. K. Monson,
854 pp. 391–414, Springer, Berlin., 2013.
- 855 Hamba, A.: Modified K model for chemically reactive species in the planetary boundary layer. *J. Geophys.*
856 *Res.*, 98 (D3), 5173–5182, doi:10.1029/92JD02511, 1993.
- 857 Hanna, S. R., Russel, A. G., Wilkinson, J. G., Vukovich, Hansen, D. A.: Monte Carlo estimation of
858 uncertainties in BEIS3 emission outputs and their effects on uncertainties in chemical transport model
859 predictions. *J. Geophys. Res.*, 110 (D01302), doi:10.1029/2004JD004986, 2005.
- 860 Harley, P., Vasconcellos, P., Vierling, L., Pinheiro, C. C. D. S., Greenberg, J., Guenther, A., Klinger, L.,
861 Almeida, S. S. De, Neill, D., Baker, T., Phillips, O., Malhi, Y. and De Almeida, S. S.: Variation in potential
862 for isoprene emissions among Neotropical forest sites, *Glob. Chang. Biol.*, 10(5), 630–650,
863 doi:10.1111/j.1529-8817.2003.00760.x, 2004.
- 864 Helmig, D., Balsley, B., Kuck, R., Jensen, M., Smith, T. and Birks, J. W.: Vertical profiling and
865 determination of landscape fluxes of biogenic nonmethane hydrocarbons within the planetary boundary layer
866 in the Peruvian Amazon, *J. Geophys. Res.*, 103(98), 519–532, doi:10.1029/98JD01023, 1998.
- 867 Jacob, D. J. and Wofsy, S. C.: Photochemistry of biogenic emissions over the Amazon forest, *J. Geophys.*
868 *Res.*, 93(D2), 1477–1486, doi:10.1029/JD093iD02p01477, 1988.
- 869 Jardine, A. B., Jardine, K. J., Fuentes, J. D., Martin, S. T., Martins, G., Durgante, F., Carneiro, V., Higuchi,
870 N., Manzi, A. O. and Chambers, J. Q.: Highly reactive light-dependent monoterpenes in the Amazon,
871 *Geophys. Res. Lett.*, 42, 1-8, doi: 10.1002/2014GL062573, 2015.
- 872 Jardine, K. J., Henderson, W. M., Huxman, T. E. and Abrell, L.: Dynamic Solution Injection: a new method
873 for preparing pptv–ppbv standard atmospheres of volatile organic compounds, *Atmos. Meas. Tech.*, 3(6),
874 1569–1576, doi:10.5194/amt-3-1569-2010, 2010.
- 875 Jardine, K. J., Monson, R. K., Abrell, L., Saleska, S. R., Arneth, A., Jardine, A., Ishida, F. Y., Serrano, A. M.
876 Y., Artaxo, P., Karl, T., Fares, S., Goldstein, A., Loreto, F. and Huxman, T.: Within-plant isoprene oxidation
877 confirmed by direct emissions of oxidation products methyl vinyl ketone and methacrolein, *Glob. Chang.*
878 *Biol.*, 18(3), 973–984, doi:10.1111/j.1365-2486.2011.02610.x, 2012.
- 879 Jardine, K., Yañez Serrano, A., Arneth, A., Abrell, L., Jardine, A., van Haren, J., Artaxo, P., Rizzo, L. V.,
880 Ishida, F. Y., Karl, T., Kesselmeier, J., Saleska, S. and Huxman, T.: Within-canopy sesquiterpene ozonolysis
881 in Amazonia, *J. Geophys. Res.*, 116(D19), D19301, doi:10.1029/2011jd016243, 2011.
- 882 Jones, M. O., Kimball, J. S. and Nemani, R. R.: Asynchronous Amazon forest canopy phenology indicates
883 adaptation to both water and light availability, *Environ. Res. Lett.*, 9(12), 124021, doi:10.1088/1748-
884 9326/9/12/124021, 2014.

- 885 Karl, T., Guenther, A., Turnipseed, A., Tyndall, G., Artaxo, P. and Martin, S.: Rapid formation of isoprene
886 photo-oxidation products observed in Amazonia, *Atmos. Chem. Phys.*, 9(20), 7753–7767, doi:10.5194/acp-9-
887 7753-2009, 2009.
- 888 Karl, T., Guenther, A., Yokelson, R. J., Greenberg, J., Potosnak, M., Blake, D. R. and Artaxo, P.: The tropical
889 forest and fire emissions experiment: Emission, chemistry, and transport of biogenic volatile organic
890 compounds in the lower atmosphere over Amazonia, *J. Geophys. Res.*, 112(D18), D18302,
891 doi:10.1029/2007JD008539, 2007.
- 892 Karl, T., Harley, P., Emmons, L., Thornton, B., Guenther, A., Basu, C., Turnipseed, A. and Jardine, K.:
893 Efficient Atmospheric Cleansing of Oxidized Organic Trace Gases by Vegetation, *Science*, 330(6005), 816–
894 819, doi:10.1126/science.1192534, 2010.
- 895 Karl, T., Potosnak, M., Guenther, A. B., Clark, D., Walker, J., Herrick, J. D. and Geron, C.: Exchange
896 processes of volatile organic compounds above a tropical rain forest: Implications for modeling tropospheric
897 chemistry above dense vegetation, *J. Geophys. Res.*, 109(D18), D18306, doi:10.1029/2004JD004738, 2004.
- 898 Kesselmeier, J., Kuhn, U., Rottenberger, S., Biesenthal, T., Wolf, A., Schebeske, G., Andreae, M. O.,
899 Ciccioli, P., Brancaleoni, E., Frattoni, M., Oliva, S. T., Botelho, M. L., Silva, C. M. A. and Tavares, T. M.:
900 Concentrations and species composition of atmospheric volatile organic compounds (VOCs) as observed
901 during the wet and dry season in Rondônia (Amazonia), *J. Geophys. Res.*, 107(D20), 8053,
902 doi:10.1029/2000JD000267, 2002.
- 903 Kesselmeier, J., Kuhn, U., Wolf, A., Andreae, M., Ciccioli, P., Brancaleoni, E., Frattoni, M., Guenther, A.,
904 Greenberg, J., De Castro Vasconcellos, P., de Oliva, T., Tavares, T. and Artaxo, P.: Atmospheric volatile
905 organic compounds (VOC) at a remote tropical forest site in central Amazonia, *Atmos. Environ.*, 34(24),
906 4063–4072, doi:10.1016/S1352-2310(00)00186-2, 2000.
- 907 Kuhn, U., Andreae, M. O., Ammann, C., Araújo, A. C., Brancaleoni, E., Ciccioli, P., Dindorf, T., Frattoni,
908 M., Gatti, L. V., Ganzeveld, L., Kruijt, B., Lelieveld, J., Lloyd, J., Meixner, F. X., Nobre, A. D., Pöschl, U.,
909 Spirig, C., Stefani, P., Thielmann, A., Valentini, R. and Kesselmeier, J.: Isoprene and monoterpene fluxes
910 from Central Amazonian rainforest inferred from tower-based and airborne measurements, and implications
911 on the atmospheric chemistry and the local carbon budget, *Atmos. Chem. Phys.*, 7(1), 641–708,
912 doi:10.5194/acpd-7-641-2007, 2007.
- 913 Kuhn, U., Rottenberger, S., Biesenthal, T., Wolf, a., Schebeske, G., Ciccioli, P., Brancaleoni, E., Frattoni, M.,
914 Tavares, T. M. and Kesselmeier, J.: Seasonal differences in isoprene and light-dependent monoterpene
915 emission by Amazonian tree species, *Glob. Chang. Biol.*, 10(5), 663–682, doi:10.1111/j.1529-
916 8817.2003.00771.x, 2004a.
- 917 Kuhn, U., Rottenberger, S., Biesenthal, T., Wolf, A., Schebeske, G., Ciccioli, P., Brancaleoni, E., Frattoni,
918 M., Tavares, T. M. and Kesselmeier, J.: Isoprene and monoterpene emissions of Amazonian tree species

- 919 during the wet season: Direct and indirect investigations on controlling environmental functions, *J. Geophys.*
920 *Res.*, 107(D20), 8071, doi:8071 10.1029/2001jd000978, 2002.
- 921 Kuhn, U., Rottenberger, S., Biesenthal, T., Wolf, A., Schebeske, G., Ciccioli, P. and Kesselmeier, J.: Strong
922 correlation between isoprene emission and gross photosynthetic capacity during leaf phenology of the tropical
923 tree species *Hymenaea courbaril* with fundamental changes in volatile organic compounds emission
924 composition during early leaf development, *Plant, Cell Environ.*, 27(12), 1469–1485, doi:10.1111/j.1365-
925 3040.2004.01252.x, 2004b.
- 926 Lamb, B., Guenther, A., Gay, D., Westberg, H.: A National Inventory of Biogenic Hydrocarbon Emissions.
927 *Atmos. Environ.*, 21(8): 1695-1705, doi:10.1016/0004-6981(87)90108-9, 1987.
- 928 Lamb, B., Pierce, T., Baldocchi, D., Allwine, E., Dilts, S., Westberg, H., Geron, C., Guenther, A., Klinger, L.,
929 Harley, P., Zimmerman, P.: Evaluation of forest canopy models for estimating isoprene emissions. *J.*
930 *Geophys. Res.*, 101(D17): 22787-22797, doi:10.1029/96JD00056, 1996.
- 931 Laothawornkitkul, J., Taylor, J. E., Paul, N. D. and Hewitt, C. N.: Biogenic volatile organic compounds in the
932 Earth system, *New Phytol.*, 183(1), 27–51, doi:10.1111/j.1469-8137.2009.02859.x, 2009.
- 933 Lelieveld, J., Butler, T. M., Crowley, J. N., Dillon, T. J., Fischer, H., Ganzeveld, L., Harder, H., Lawrence, M.
934 G., Martinez, M., Taraborrelli, D. and Williams, J.: Atmospheric oxidation capacity sustained by a tropical
935 forest, *Nature*, 452(7188), 737–40, doi:10.1038/nature06870, 2008.
- 936 Lima, P., Zoghbi, G. B., Andrade, E. H. A., D, T. M., Fernandes, C. S., Lauraceae, B. and Words, K. E. Y.:
937 Constituintes voláteis das folhas e dos galhos de *Cinnamomum zeylanicum* Blume (Lauraceae) Volatile
938 constituents from leaves and branches of, *Acta Amaz.*, 35(3), 363–366, 2005.
- 939 Lindinger, W., Hansel, A. and Jordan, A.: On-line monitoring of volatile organic compounds at pptv levels by
940 means of proton-transfer-reaction mass spectrometry (PTR-MS) medical applications, food control and
941 environmental research, *Int. J. Mass Spectrom. Ion Process.*, 173(3), 191–241,
942 doi:http://dx.doi.org/10.1016/S0168-1176(97)00281-4, 1998.
- 943 Liu, Y. J., Herdinger-Blatt, I., McKinney, K. a. and Martin, S. T.: Production of methyl vinyl ketone and
944 methacrolein via the hydroperoxyl pathway of isoprene oxidation, *Atmos. Chem. Phys.*, 13, 5715–5730,
945 doi:10.5194/acp-13-5715-2013, 2013.
- 946 Loreto, F., Ciccioli, P., Cecinato, A., Brancaleoni, E., Frattoni, M., Fabozzi, C., Tricoli, D., C, C. I. A. P. and
947 Salaria, V.: Evidence of the Photosynthetic Origin of Monoterpenes Emitted by *Quercus ilex* L. Leaves by
948 I3C Labeling, *Plant Physiol.*, 110(1996), 1317–1322, 1996.
- 949 Loreto, F. and Velikova, V.: Isoprene produced by leaves protects the photosynthetic apparatus against ozone
950 damage, quenches ozone products, and reduces lipid peroxidation of cellular membranes, *Plant Physiol.*,
951 127(4), 1781–7, doi:10.1104/pp.010497., 2001.

- 952 Luizão, F. J.: Litter production and mineral element input to the forest floor in a central Amazonian forest,
953 *GeoJournal*, 19(4), 407-417, 1989.
- 954 Malhi, Y., Aragão, L. E. O. C., Metcalfe, D. B., Paiva, R., Quesada, C. A., Almeida, S., Anderson, L.,
955 Brando, P., Chambers, J. Q., da COSTA, A. C. L., Hutyra, L. R., Oliveira, P., Patiño, S., Pyle, E. H.,
956 Robertson, A. L. and Teixeira, L. M.: Comprehensive assessment of carbon productivity, allocation and
957 storage in three Amazonian forests, *Glob. Chang. Biol.*, 15(5), 1255–1274, doi:10.1111/j.1365-
958 2486.2008.01780.x, 2009.
- 959 Marengo, J. A., Nobre, C. A., Tomasella, J., Oyama, M. D., Sampaio de Oliveira, G., de Oliveira, R.,
960 Camargo, H., Alves, L. M. and Brown, I. F.: The Drought of Amazonia in 2005, *J. Clim.*, 21(3), 495–516,
961 doi:10.1175/2007JCLI1600.1, 2008.
- 962 Marengo, J. A., Tomasella, J., Alves, L. M., Soares, W. R. and Rodriguez, D. A.: The drought of 2010 in the
963 context of historical droughts in the Amazon region, *Geophys. Res. Lett.*, 38(12), 1-5,
964 doi:10.1029/2011GL047436, 2011.
- 965 Martin, S. T., Andreae, M. O., Althausen, D., Artaxo, P., Baars, H., Borrmann, S., Chen, Q., Farmer, D. K.,
966 Guenther, A., Gunthe, S. S., Jimenez, J. L., Karl, T., Longo, K., Manzi, A., Muller, T., Pauliquevis, T.,
967 Petters, M. D., Prenni, A. J., Poschl, U., Rizzo, L. V, Schneider, J., Smith, J. N., Swietlicki, E., Tota, J.,
968 Wang, J., Wiedensohler, A. and Zorn, S. R.: An overview of the Amazonian Aerosol Characterization
969 Experiment 2008 (AMAZE-08), *Atmos. Chem. Phys.*, 10(23), 11415–11438, doi:10.5194/acp-10-11415-
970 2010, 2010.
- 971 Misztal, P. K., Karl, T., Weber, R., Jonsson, H. H., Guenther, A. B., Goldstein, A., H.: Airborne flux
972 measurements of biogenic isoprene over California. *Atmos. Chem. Phys.*, 14(19): 10631-10647,
973 doi:10.5194/acp-14-10631-2014, 2014.
- 974 MODIS-NASA: Leaf Area Index - Fraction Photosynth. Act. Radiat. 8-Day L4 Glob. 1km [online] Available
975 from: https://lpdaac.usgs.gov/dataset_discovery/modis/modis_products_table/mcd15a2, 2015.
- 976 Monson, R. K., Grote, R., Niinemets, Ü. and Schnitzler, J.-P.: Modeling the isoprene emission rate from
977 leaves, 195, 541–559, doi:10.1111/j.1469-8137.2012.04204.x, 2012.
- 978 Morfopoulos, C., Prentice, I. C., Keenan, T. F., Friedlingstein, P., Medlyn, B. E., Peñuelas, J. and Possell, M.:
979 A unifying conceptual model for the environmental responses of isoprene emissions from plants, *Ann. Bot.*,
980 112(7), 1223–38, doi:10.1093/aob/mct206, 2013.
- 981 Morfopoulos, C., Sperlich, D., Pe, J., Filella, I., Llusi, J., Possell, M., Sun, Z., Prentice, I. C. and Medlyn, B.
982 E.: A model of plant isoprene emission based on available reducing power captures responses to atmospheric
983 CO₂, *New Phytol.*, 203 , 125–139, doi: 10.1111/nph.12770,2014.

- 984 Morton, D. C., Nagol, J., Carabajal, C. C., Rosette, J., Palace, M., Cook, B. D., Vermote, E. F., Harding, D. J.
985 and North, P. R. J.: Amazon forests maintain consistent canopy structure and greenness during the dry season,
986 *Nature*, 506(7487), 221–4, doi:10.1038/nature13006, 2014.
- 987 Müller, J. F., Stavrakou, T., Wallens, S., De Smedt, I., Van Roozendael, M., Potosnak, M. J., Rinne, J.,
988 Munger, B., Goldstein, A., Guenther, A. B., Smedt, I. De and Roozendael, M. Van: Global isoprene emissions
989 estimated using MEGAN, ECMWF analyses and a detailed canopy environment model, *Atmos. Chem. Phys.*,
990 8(5), 1329–1341, doi:10.5194/acp-8-1329-2008, 2008.
- 991 Myneni, R. B., Yang, W., Nemani, R. R., Huete, A. R., Dickinson, R. E., Knyazikhin, Y., Didan, K., Fu, R.,
992 Negrón Juárez, R. I., Saatchi, S. S., Hashimoto, H., Ichii, K., Shabanov, N. V, Tan, B., Ratana, P., Privette, J.
993 L., Morisette, J. T., Vermote, E. F., Roy, D. P., Wolfe, R. E., Friedl, M. A., Running, S. W., Votava, P., El-
994 Saleous, N., Devadiga, S., Su, Y. and Salomonson, V. V: Large seasonal swings in leaf area of Amazon
995 rainforests, *Proc. Natl. Acad. Sci. U. S. A.*, 104(12), 4820–4823, doi:10.1073/pnas.0611338104, 2007.
- 996 Nelson, B., Tavares, J., Wu, J., Valeriano, D., Lopes, A., Marostica, S., Martins, G., Prohaska, N., Albert, L.,
997 De Araújo, A., Manzi, A., Saleska, S., Huete, A.: Seasonality of central Amazon Forest Leaf Flush using
998 tower mounted RGB Camera, AGU Fall Meeting, San Francisco, California, 15-19 December, B11G-0107,
999 2014.
- 1000 Nemitz, E., Sutton, M. A., Gut, A., San José, R., Husted, S. and Schjoerring, J. K.: Sources and sinks of
1001 ammonia within an oilseed rape canopy, *Agric. For. Meteorol.*, 105(4), 385–404, doi:10.1016/S0168-
1002 1923(00)00205-7, 2000.
- 1003 Oliveira, A. N. De, Braule, M., Ramos, P., Couto, L. B. and Sahdo, R. M.: Composição e diversidade
1004 florístico-estrutural de um hectare de floresta densa de terra firme na Amazônia, *Acta Amaz.*, 38(4), 627–642,
1005 doi: 10.1590/S0044-59672008000400005, 2008.
- 1006 Park, J.-H., Goldstein, A. H., Timkovsky, J., Fares, S., Weber, R., Karlik, J. and Holzinger, R.: Active
1007 atmosphere-ecosystem exchange of the vast majority of detected volatile organic compounds, *Science*,
1008 341(6146), 643–647, doi:10.1126/science.1235053, 2013.
- 1009 Parker, G., and D. R. Fitzjarrald.: Canopy structure and radiation environment metrics indicate forest
1010 developmental stage, disturbance, and certain ecosystem functions, III LBA Scientific Conference, Braz.
1011 Minist. of Sci. and Technol., Brasilia, Brazil, 27-29 July, 2004.
- 1012 Pires, J. M. and Prance, G. T.: Key environments: Amazonia, in *Vegetation types of the Brazilian Amazonia.*,
1013 edited by G. T. Prance and T. E. Lovejoy, Pergamon, New York., 1985.
- 1014 Rasmussen, R. A. and Khalil, M. A. K.: Isoprene over the Amazon Basin, *J. Geophys. Res.*, 93(D2), 1417,
1015 doi:10.1029/JD093iD02p01417, 1988.
- 1016 Raupach, M.: Applying Lagrangian Fluid Mechanics to infer scalar source distributions from concentration
1017 profiles in plant canopies, *Agric. For. Meteorol.*, 47, 85–108, doi:10.1016/0168-1923(89)90089-0, 1989.

- 1018 Restrepo-Coupe, N., da Rocha, H. R., Hutyrá, L. R., da Araujo, A. C., Borma, L. S., Christoffersen, B.,
1019 Cabral, O. M. R. R., de Camargo, P. B., Cardoso, F. L., da Costa, A. C. L., Fitzjarrald, D. R., Goulden, M. L.,
1020 Kruijt, B., Maia, J. M. F. F., Malhi, Y. S., Manzi, A. O., Miller, S. D., Nobre, A. D., von Randow, C., Sá, L.
1021 D. A., Sakai, R. K., Tota, J., Wofsy, S. C., Zanchi, F. B. and Saleska, S. R.: What drives the seasonality of
1022 photosynthesis across the Amazon basin? A cross-site analysis of eddy flux tower measurements from the
1023 Brasil flux network, *Agric. For. Meteorol.*, 182-183, 128–144, doi:10.1016/j.agrformet.2013.04.031, 2013.
- 1024 Rinne, H. J. I., Guenther, A. B., Greenberg, J. P. and Harley, P. C.: Isoprene and monoterpene fluxes
1025 measured above Amazonian rainforest and their dependence on light and temperature, *Atmos. Environ.*,
1026 36(14), 2421–2426, doi:10.1016/S1352-2310(01)00523-4, 2002.
- 1027 Rizzo, L. V. V., Artaxo, P., Karl, T., Guenther, A. B. B. and Greenberg, J.: Aerosol properties, in-canopy
1028 gradients, turbulent fluxes and VOC concentrations at a pristine forest site in Amazonia, *Atmos. Environ.*,
1029 44(4), 503–511, doi:10.1016/j.atmosenv.2009.11.002, 2010.
- 1030 Samanta, A., Knyazikhin, Y., Xu, L., Dickinson, R. E., Fu, R., Costa, M. H., Saatchi, S. S., Nemani, R. R. and
1031 Myneni, R. B.: Seasonal changes in leaf area of Amazon forests from leaf flushing and abscission, *J.*
1032 *Geophys. Res. Biogeosciences*, 117(G1), n/a–n/a, doi:10.1029/2011JG001818, 2012.
- 1033 Silva, C. P.: Estudos observacionais das principais fontes de emissão de compostos orgânicos voláteis (VOC)
1034 em floresta intacta de terra firme na Amazônia Central [*in Portuguese*], Master thesis. National Institute for
1035 Amazon Research, Manaus-AM, Brazil, 91 pp., 2010.
- 1036 Silva, F. B., Shimabukuro, Y. E., Aragão, L. E. O. C., Anderson, L. O., Pereira, G., Cardozo, F. and Arai, E.:
1037 Corrigendum: Large-scale heterogeneity of Amazonian phenology revealed from 26-year long
1038 AVHRR/NDVI time-series, *Environ. Res. Lett.*, 8(2), 029502, doi:10.1088/1748-9326/8/2/029502, 2013.
- 1039 Simon, E., Meixner, F. X., Rummel, U., Ganzeveld, L., Ammann, C. and Kesselmeier, J.: Coupled carbon-
1040 water exchange of the Amazon rain forest, II. Comparison of predicted and observed seasonal exchange of
1041 energy, CO₂, isoprene and ozone at a remote site in Rondonia, *Biogeosciences*, 2(3), 255–275,
1042 doi:10.5194/bg-2-255-2005, 2005.
- 1043 Stark, S. C., Leitold, V., Wu, J. L., Hunter, M. O., de Castilho, C. V., Costa, F. R. C., McMahon, S. M.,
1044 Parker, G. G., Shimabukuro, M. T., Lefsky, M. a, Keller, M., Alves, L. F., Schiatti, J., Shimabukuro, Y. E.,
1045 Brandão, D. O., Woodcock, T. K., Higuchi, N., de Camargo, P. B., de Oliveira, R. C., Saleska, S. R. and
1046 Chave, J.: Amazon forest carbon dynamics predicted by profiles of canopy leaf area and light environment.,
1047 *Ecol. Lett.*, 15(12), 1406–14, doi:10.1111/j.1461-0248.2012.01864.x, 2012.
- 1048 Stavrou, T., Müller, J.-F., Bauwens, M., De Smedt, I., Van Roozendael, M., De Mazière, M., Vigouroux,
1049 C., Hendrick, F., George, M., Clerbaux, C., Coheur, P.-F. and Guenther, A.: How consistent are top-down
1050 hydrocarbon emissions based on formaldehyde observations from GOME-2 and OMI? *Atmos. Chem. Phys.*
1051 *Discuss.*, 15, 12007-12067, doi:10.5194/acpd-15-12007-2015, 2015.

- 1052 Stavrakou, T., Müller, J.-F., Bauwens, M., De Smedt, I., Van Roozendael, M., Guenther, A., Wild, M. and
1053 Xia, X.: Isoprene emissions over Asia 1979–2012: impact of climate and land-use changes, *Atmos. Chem.*
1054 *Phys.*, 14(9), 4587–4605, doi:10.5194/acp-14-4587-2014, 2014.
- 1055 Stavrakou, T., Müller, J.-F., De Smedt, I., Van Roozendael, M., van der Werf, G. R., Giglio, L. and Guenther,
1056 a.: Global emissions of non-methane hydrocarbons deduced from SCIAMACHY formaldehyde columns
1057 through 2003–2006, *Atmos. Chem. Phys.*, 9, 3663–3679, 2009, doi:10.5194/acp-9-3663-2009, 2009.
- 1058 Stefani, P.: Preliminary assessment of VOC fluxes from a primary rain forest performed in the LBA site at
1059 Manaus, I LBA Scientific Conference, Braz. Minist. of Sci. and Technol., Belém, Brazil, 2-4 June, 2000.
- 1060 Tavares, J. V.: Green-up na Estação Seca da Amazônia Central: Padrões sazonais da fenologia foliar de uma
1061 floresta de terra firme [*in Portuguese*]. Master thesis. National Institute for Amazon Research, Manaus-AM,
1062 Brazil, 40 pp., 2013.
- 1063 Trostdorf, C. R., Gatti, L. V., Yamazaki, a., Potosnak, M. J., Guenther, A., Martins, W. C. and Munger, J. W.:
1064 Seasonal cycles of isoprene concentrations in the Amazonian rainforest, *Atmos. Chem. Phys. Discuss.*, 4(2),
1065 1291–1310, doi:10.5194/acpd-4-1291-2004, 2004.
- 1066 Unger, N., Harper, K., Zheng, Y., Kiang, N. Y., Aleinov, I., Arneth, a., Schurgers, G., Amelynck, C.,
1067 Goldstein, A., Guenther, A., Heinesch, B., Hewitt, C. N., Karl, T., Laffineur, Q., Langford, B., A. McKinney,
1068 K., Misztal, P., Potosnak, M., Rinne, J., Pressley, S., Schoon, N. and Serça, D.: Photosynthesis-dependent
1069 isoprene emission from leaf to planet in a global carbon-chemistry-climate model, *Atmos. Chem. Phys.*,
1070 13(20), 10243–10269, doi:10.5194/acp-13-10243-2013, 2013.
- 1071 Warneke, C., Gouw, J. A., Del Negro, L., Brioude, J., Mckeen, S., Stark, H., Kuster, W. C., Goldan, P. D.,
1072 Trainer, M., Fehsenfeld, F. C., Wiedinmyer, C., Guenther, A., B., Hansel, A., Wisthaler, A., Atlas, E.,
1073 Holloway, J. S., Ryerson, T. B., Peischl, j., Huey, L. G., Case Hanks, A. T.: Biogenic emission measurement
1074 and inventories determination of biogenic emissions in the eastern United States and Texas and comparison
1075 with biogenic emission inventories. *J. Geophys. Res.*, 115(D00F18), doi:10.1029/2009JD012445, 2010.
- 1076 Yáñez-Serrano, A. M., Nölscher, A C., Williams, J., Wolff, S., Alves, E., Martins, G. a, Bourtsoukidis, E.,
1077 Brito, J., Jardine, K. J., Artaxo, P. and Kesselmeier, J.: Diel and seasonal changes of biogenic volatile organic
1078 compounds within and above an Amazonian rainforest, *Atmos. Chem. Phys.*, 15, 3359–3378,
1079 doi:10.5194/acp-15-3359-2015, 2015.
- 1080 Zimmerman, P. R., Greenberg, J. P. and Westberg, C. E.: Measurements of atmospheric hydrocarbons and
1081 biogenic emission fluxes in the Amazon Boundary layer, *J. Geophys. Res.*, 93(D2), 1407,
1082 doi:10.1029/JD093iD02p01407, 1988.

Table1: Isoprene and monoterpenes from different regions in the Amazonian rainforest: comparison of estimates and direct measurements of mixing ratios and fluxes.

Study	Site	Technical approach	isoprene (ppbv)	isoprene (mg m ⁻² h ⁻¹)	sum of Mt [†] (ppbv)	sum of Mt [†] (mg m ⁻² h ⁻¹)	season	comments
Central Amazonia								
Greenberg and Zimmerman, 1984	Manaus/Humaitá-Amazonas, Brazil	GC-FID, canister samples (near ground to 30m)	2.40 (1-5.24) ^a		2.86		Dry (Aug-Sep 1980)	mean - daytime range i not reported
Greenberg and Zimmerman, 1984	Manaus/Humaitá-Amazonas, Brazil	GC-FID, canister samples (flights from treetop to 2 km)	2.27 (0.38-4.08) ^a		5.47		Dry (Aug-Sep 1980)	mean - daytime range i not reported
Greenberg and Zimmerman, 1984	Manaus/Humaitá-Amazonas, Brazil	GC-FID canister samples (flights from 2km to Tropopause)	0.19 (0.14-0.22) ^a		1.91		Dry (Aug-Sep 1980)	mean - daytime range i not reported
Jacob and Wofsy, 1988*	ABLE - Adolfo Ducke Forest Reserve - Manaus-Amazonas, Brazil	Inverse modeling approach using Zimmerman et al. 1988 data		1.58			Dry (July-Aug 1985)	mean average of 24 hour
Zimmerman et al., 1988*	ABLE - Adolfo Ducke Forest Reserve - Manaus-Amazonas, Brazil	GC-FID, teflon bag on tethered balloon (30m)	2.65 [1.39-3.38] ^b		0.27 [0.15-0.54] ^b		Dry (July-Aug 1985)	median and interquartil range (24h)
Zimmerman et al., 1988*	ABLE - Adolfo Ducke Forest Reserve - Manaus-Amazonas, Brazil	GC-FID, teflon bag on tethered balloon (305m)	1.73 [1.03-2.15] ^b		0.15 [0.04-0.33] ^b		Dry (July-Aug 1985)	median and interquartil range (24h)
Zimmerman et al., 1988*	ABLE - Adolfo Ducke Forest Reserve - Manaus-Amazonas, Brazil	GC-FID, teflon bag on tethered balloon (up to 305m)		3.1		0.23	Dry (July-Aug 1985)	mean daytime (08:00 16:00, LT)
Rasmussen and Khalil, 1988	ABLE - Adolfo Ducke Forest Reserve - Manaus-Amazonas, Brazil	GC-FID, canister samples (near ground level)	2.77 (±0.4)				Dry (July-Aug 1985)	mean daytime (11:00 15:00, LT)
Rasmussen and Khalil, 1988	ABLE - Adolfo Ducke Forest Reserve - Manaus-Amazonas, Brazil	GC-FID, canister samples (aircraft flights from 150m to 5000m)	1.5 (±0.75)				Dry (July-Aug 1985)	daytime
Davis et al., 1994*	ABLE - Adolfo Ducke Forest Reserve - Manaus-Amazonas, Brazil	Mixed Layer Gradient approach using Zimmerman et al. 1988 data		3.63 (±1.4)			Dry (July-Aug 1985)	mean daytime (08:00 18:00, LT)
Kesselmeier et al., 2000	Balbina - ~100 km north of Manaus-Amazonas, Brazil	GC-MS, cartridge samples (outside forest)	6.55 (±1.26)		0.63 (±0.19)		Wet (Apr 1988)	mean daytime (09:30 15:00, LT)
		GC-MS, cartridge samples (inside Canopy)	3.55 (±0.07)		0.24 (±0.04)		Wet (Apr 1988)	mean daytime (09:30 15:00, LT)
		GC-MS, cartridge on tethered balloon (200-500m)	~3		~0.2		Wet (Apr 1988)	mean of 24h

Cont. Table1: Isoprene and monoterpenes from different regions in the Amazonian rainforest: comparison of estimates and direct measurements of mixing ratios and fluxes.

study	Site	Technical approach	isoprene (ppbv)	isoprene (mg m ⁻² h ⁻¹)	sum of Mt [†] (ppbv)	sum of Mt [†] (mg m ⁻² h ⁻¹)	season	comments
Central Amazonia								
Kesselmeier et al., 2000	Cuieiras Biological Reserve (C14-ZF2) - Manaus-Amazonas, Brazil	GC-MS, cartridge samples (inside and above canopy)	6.7 ±1.07		0.73 ±0.24		Wet (Apr 1988)	daytime
Stefani et al. 2000	Cuieiras Biological Reserve (K34-ZF2) - Manaus-Amazonas, Brazil	GC-MS, cartridge on Relaxed Eddy Accumulation (~53m)		3.6 -5.4		0.72 – 0.9	Aug 1999 and Jan 2000	range of daytime averaged normalized fluxes for the whole period of measurement
Andreae et al., 2002	Cuieiras Biological Reserve (K34-ZF2) - Manaus-Amazonas, Brazil	GC-MS, cartridge on Relaxed Eddy Accumulation (~53m)		2.88		0.36	Dry-Wet (Nov 1999-Jan 2000)	midday values
Diccioli et al., 2003	Cuieiras Biological Reserve (K34-ZF2) - Manaus-Amazonas, Brazil	GC-MS, cartridge on Relaxed Eddy Accumulation (~51m)		5.11 max.		1.36 max.	Dry (July 2001)	midday values
Greenberg et al., 2004	Balbina - ~100 km north of Manaus-Amazonas, Brazil	GC-MS, cartridge on tethered balloon (200-1000m)	2.86 [2.25-3.64] ^b		0.21 [0.17-0.31] ^b		Wet (March 1998)	median and interquartiles daytime (12:00-15:00, LT)
Greenberg et al., 2004	Balbina - ~100 km north of Manaus-Amazonas, Brazil	Box model		5.3		0.23	Wet (March 1998)	maximum midday emission fluxes estimated for the ecoregion
Karl et al., 2007 ^{††}	Cuieiras Biological Reserve (C14-ZF2) - Manaus-Amazonas, Brazil	PTR-MS, Disjunct Eddy Covariance (~ 54 m)	7.8 ±3.7	8.3 ±3.1	0.87 ±0.3	1.7 ±1.3	Dry (Sep 2004)	mean daytime (12:00-14:00 LT)
Karl et al., 2007 ^{††}	Cuieiras Biological Reserve (C14-ZF2) - Manaus-Amazonas, Brazil	PTR-MS, Mixed Layer Gradient (up to ~1200 m)	5.5 ±2.6	12.1 ±4.0	0.52 ±0.2	3.5 ±1.2	Dry (Sep 2004)	mean daytime (10:00-11:30 LT)
Kuhn et al., 2007 ^{**}	Cuieiras Biological Reserve (K34-ZF2)- Manaus-Amazonas, Brazil	GC-FID, cartridge on Relaxed Eddy Accumulation (~51m)		2.4 ±1.8 (max. 6.1)		0.44 ±0.49 (max. 1.9)	Dry (July 2001)	mean daytime (10:00-15:00 LT)
Kuhn et al., 2007 ^{**}	Cuieiras Biological Reserve (K34-ZF2) - Manaus-Amazonas, Brazil	GC-FID, cartridge on Surface Layer Gradient (28, 35.5, 42.5, 51m)		3.9 ±4.1 (max. 12.8)		0.43 ±0.65 (max. 2.1)	Dry (July 2001)	mean daytime (10:00-15:00 LT)
Kuhn et al., 2007 ^{**}	Cuieiras Biological Reserve (K34-ZF2) - Manaus-Amazonas, Brazil	GC-FID, cartridge samples, Mixed Layer Gradient (50-3000m)		4.2 ±5.9 (max. 15.7)			Dry (July 2001)	mean daytime (10:00-18:00 LT)
Karl et al., 2009	Cuieiras Biological Reserve (TT34-ZF2) - Manaus-Amazonas, Brazil	PTR-MS, Gradient flux (2, 10.9, 16.7, 23.9, 30.3 and 39.8 m)		0.7 ±0.2			Wet (Feb 2008)	mean daytime (11:00-17:00 LT); flux at 35 m
Rizzo et al., 2010 ^{††}	Cuieiras Biological Reserve (C14-ZF2)- Manaus-Amazonas,	PTR-MS, Disjunct Eddy Covariance (54 m)	7.8		0.29		Dry (Sep 2004)	max. at early afternoon
				8.4		0.93	Dry (Sep 2004)	max. at noon

Cont. Table1: Isoprene and monoterpenes from different regions in the Amazonian rainforest: comparison of estimates and direct measurements of mixing ratios and fluxes.

study	Site	Technical approach	isoprene (ppbv)	isoprene (mg m ⁻² h ⁻¹)	sum of Mt [†] (ppbv)	sum of Mt [†] (mg m ⁻² h ⁻¹)	season	comments
Central Amazonia								
Silva, 2010	Cuieiras Biological Reserve (K34-ZF2)-Manaus-Amazonas, Brazil	GC-MSFID cartridge samples at 1m	3.2 ±0.9		0.28 ±0.13		Wet (May 2009)	mean daytime (07:00-17:00 LT)
		GC-MSFID cartridge samples at 10m	4.6 ±0.94		1.09 ±0.35		Wet (May 2009)	mean daytime (07:00-17:00 LT)
		GC-MSFID cartridge samples at 20m	6.17 ±1.03		0.75 ±0.17		Wet (May 2009)	mean daytime (07:00-17:00 LT)
Cardine et al., 2011 [‡]	Cuieiras Biological Reserve (TT34-ZF2)-Manaus-Amazonas, Brazil	PTR-MS, Gradient profile (2, 11, 17, 24, 30 and 40 m)			~ 0.78		Dry-Wet (Sep-Dec 2010)	mean daytime 10:00-16:00 LT) at 40 m
Cardine et al., 2011 [‡]	Cuieiras Biological Reserve (TT34-ZF2)-Manaus-Amazonas, Brazil	PTR-MS, Gradient profile (2, 11, 17, 24, 30 and 40 m)				~ 1.47	Dry-Wet (Sep-Dec 2010)	mean daytime 10:00-16:00 LT) at 35 m
Cardine et al., 2012 [‡]	Cuieiras Biological Reserve (TT34-ZF2)-Manaus-Amazonas, Brazil	PTR-MS, Gradient profile (2, 11, 17, 24, 30 and 40 m) and Gradient flux		~1.43			Dry-Wet (Sep-Dec 2010)	mean daytime (10:00-16:00 LT); flux at 40 m
Yáñez-Serrano et al., 2015	ATTO site - Manaus Manaus-Amazonas, Brazil	PTR-MS, Gradient profile (0.05, 0.5, 4, 24, 38, 53 and 79 m)	5.22 ±1.5		0.75 ±0.18		Dry (Sep 2013)	Isoprene, daytime median (12 15:00, LT). Mt, daytime median (15-18:00, LT)
Yáñez-Serrano et al., 2015	ATTO site - Manaus Manaus-Amazonas, Brazil		1.5 ±0.78		< 0.23		Wet (Feb-Mar 2013)	Isoprene, daytime median (12 15:00, LT). Mt, daytime median (15-18:00, LT)
This study [‡]	Cuieiras Biological Reserve (TT34-ZF2) - Manaus-Amazonas, Brazil	PTR-MS, Gradient profile (2, 11, 17, 24, 30 and 40 m) and Gradient flux	2.68 ±0.9	1.37 ±0.7	0.67 ±0.3	1.47 ±0.06	Dry (Sep-Oct 2010)	mean daytime (10:00-14:00, LT) at 40m
This study [‡]	Cuieiras Biological Reserve (TT34-ZF2) - Manaus-Amazonas, Brazil	PTR-MS, Gradient profile (2, 11, 17, 24, 30 and 40 m) and Gradient flux	2.65 ±1.33	1.41 ±0.1	0.85 ±0.4	1.29 ±0.2	DWT [§] (Nov 2010)	mean daytime (10:00-14:00, LT) at 40m
This study [‡]	Cuieiras Biological Reserve (TT34-ZF2) - Manaus-Amazonas, Brazil	PTR-MS, Gradient profile (2, 11, 17, 24, 30 and 40 m) and Gradient flux	1.66 ±0.9	0.52 ±0.1	0.47 ±0.2	0.36 ±0.05	Wet (Dec 2010 -Jan 2011)	mean daytime (10:00-14:00, LT) at 40m
Eastern central Amazonia								
Rinne et al., 2002	Tapajós National Forest - Santarém-Pará, Brazil	GC-MS cartridge on Disjunct Eddy Accumulation (~ 45m)	5 max.	2.4			Dry (July 2000)	Afternoon values 30 °C and 1000 μmol m ⁻² s ⁻¹
Greenberg et al., 2004	Tapajós National Forest - Santarém-Pará, Brazil	GC-MS, cartridge on tethered balloon (200-1000m)	0.74 [0.6-1] ^b		0.08 [0.03-0.06] ^b		Wet (Jan-Feb 2000)	median and interquartiles daytime (12:00-15:00, LT)
Greenberg et al., 2004	Tapajós National Forest - Santarém-Pará, Brazil	Box model		2.2		0.18	Wet (Jan-Feb 2000)	maximum midday emission fluxes estimated for the ecoregion

Cont. Table1: Isoprene and monoterpenes from different regions in the Amazonian rainforest: comparison of estimates and direct measurements of mixing ratios and fluxes.

study	Site	Technical approach	isoprene (ppbv)	isoprene ($\text{mg m}^{-2} \text{h}^{-1}$)	sum of Mt^{\dagger} (ppbv)	sum of Mt^{\dagger} ($\text{mg m}^{-2} \text{h}^{-1}$)	season	comments
Eastern central Amazonia								
Frostdorf et al., 2004	Tapajós National Forest - Santarém-Pará, Brazil	GC-FID, canister samples (54, 64 m)	1.9 \pm 1.2; 1.3 \pm 0.8				Wet (Jan- May 2002)	mean daytime (11:00-14:00 LT)
Frostdorf et al., 2004	Tapajós National Forest - Santarém-Pará, Brazil	GC-FID, canister samples (54, 64 m)	1.4 \pm 0.5; 1.0 \pm 0.4				WDT ^{WY} (June- July 2002)	mean daytime (11:00-14:00 LT)
Frostdorf et al., 2004	Tapajós National Forest - Santarém-Pará, Brazil	GC-FID, canister samples (54, 64 m)	2.8 \pm 0.9; 2.5 \pm 0.8				Dry (Aug-Nov 2002)	mean daytime (11:00-14:00 LT)
Western Amazonia								
Helmig et al., 1998	Peru - 500 km west of Iquitos	GC-MS, cartridge on tethered balloon (up to 1600 m)	3.31, 1.39, 0.16		0.21, 0.06, 0.015		July 1996	Median daytime (ground mixed layer and above mixed layer)
Helmig et al., 1998	Peru - 500 km west of Iquitos	GC-MS, cartridge samples, Mixed Layer Gradient		7.4		0.42		mean daytime
Helmig et al., 1998	Peru - 500 km west of Iquitos	GC-MS, cartridge samples, Mixed Layer Budget		8.1		0.41		mean daytime
Southern Amazonia								
Kesselmeier et al., 2002	Jaru Biological Reserve, Rondônia, Brazil	GC-FID, cartridge samples (8-52m)	~4		~0.8		WDT ^{WY} (May 1999)	mean daytime (11:00-18:00 LT)
Kesselmeier et al., 2002	Jaru Biological Reserve, Rondônia, Brazil	GC-FID, cartridge samples (8-52m)	~12		~0.8		DWT ^Y (Sep- Out 1999)	mean daytime (11:00-18:00 LT)
Greenberg et al., 2004	Jaru Biological Reserve, Jaru-Rondônia, Brazil	GC-MS, cartridge on tethered balloon (200-1000m)	6.89 [2.78-7.73] ^b		0.83 [0.56-2.65] ^b		Wet (Feb 1999)	median and interquartiles daytime (12:00-15:00, LT)
Greenberg et al., 2004	Jaru Biological Reserve, Jaru-Rondônia, Brazil	Box model		9.8		6.1	Wet (Feb 1999)	maximum midday emission fluxes estimated for the ecoregion
Simon et al., 2005	Jaru Biological Reserve, Rondônia, Brazil	Lagrangian transport sub-model.		~5.9			WDT ^{WY} (May 1999)	midday values
Simon et al., 2005	Jaru Biological Reserve, Rondônia, Brazil	Modeling using data of Kesselmeier et al., 2002		~8.2			DWT ^Y (Sep- Out 1999)	midday values

Cont. Table1: Isoprene and monoterpenes from different regions in the Amazonian rainforest: comparison of estimates and direct measurements of mixing ratios and fluxes.

study	Site	Technical approach	isoprene (ppbv)	isoprene (mg m ⁻² h ⁻¹)	sum of Mt [†] (ppbv)	sum of Mt [†] (mg m ⁻² h ⁻¹)	season	comments
southern Amazonia								
Aquino, 2006	Jaru Biological Reserve, Rondônia, Brazil	GC-FID, canister samples (50, 60 m)	4.5 ±0.9; 4.0 ±1.2				Wet (Feb-May 2002)	mean daytime (11:00-16:00 LT)
Aquino, 2006	Jaru Biological Reserve, Rondônia, Brazil	GC-FID, canister samples (50, 60 m)	2.1 ±2.0; 1.8 ±1.8				WDT ^{yy} (Jun 2002)	mean daytime (11:00-16:00 LT)
Aquino, 2006	Jaru Biological Reserve, Rondônia, Brazil	GC-FID, canister samples (50, 60 m)	4.6 ±2.7; 4.0 ±2.5				Dry (Jul-Sep 2002)	mean daytime (11:00-16:00 LT)
Aquino, 2006	Jaru Biological Reserve, Rondônia, Brazil	GC-FID, canister samples (50, 60 m)	3.4 ±1.2; 3.0 ±0.5				DWT ^y (Out- Nov 2002)	mean daytime (11:00-16:00 LT)

Note: Seasons follow determination of each study. For some studies the exact times of sample collection are not available and then not reported. Statistics differed among studies. The most of studies showed mean values but others presented median values and/or just a range of all values measured.

†Mt - monoterpenes;

^a - range of variation;

^b - interquartile ranges based on median "[]";

* ** studies derived from the same observational data base;

‡ †† studies derived from part of the same observational data base;

^yDWT - dry-to-wet transition season;

^{yy}WDT - wet-to-dry transition season.

Figures

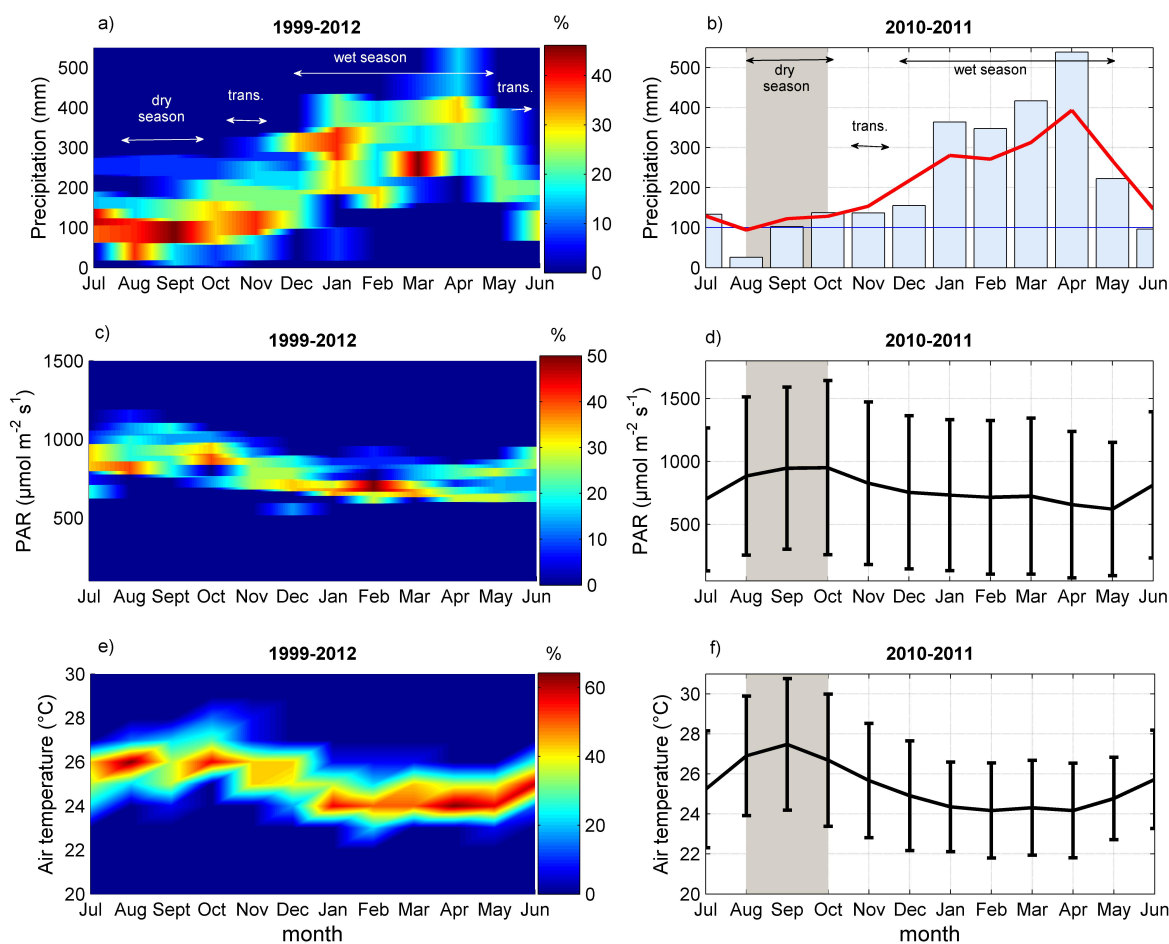


Figure 1: Precipitation, PAR and air temperature measured at K34 tower (~2 km far of TT34 tower); a) relative frequency (%) of monthly cumulative precipitation from 1999 to 2012, b) monthly cumulative precipitation from July 2010 to June 2011 (measured in 30 minute intervals for 24 hours) (bars), and average of monthly cumulative precipitation from 1999 to 2012 (red line); c) relative frequency of monthly PAR from 1999 to 2012 (measured every 30 min during 06:00-18:00, LT), d) monthly average PAR from July 2010 to June 2011 (measured every 30 min during 06:00-18:00, LT); e) relative frequency of monthly air temperature from 1999 to 2012, f) monthly average air temperature from July 2010 to June 2011 (measured in 30 minute intervals for 24 hours). Figures on the right side cover the period of this study; grey areas represent the period of dry season; and blue line at (b) represents 100 mm month⁻¹. Error bars represent one standard deviation.

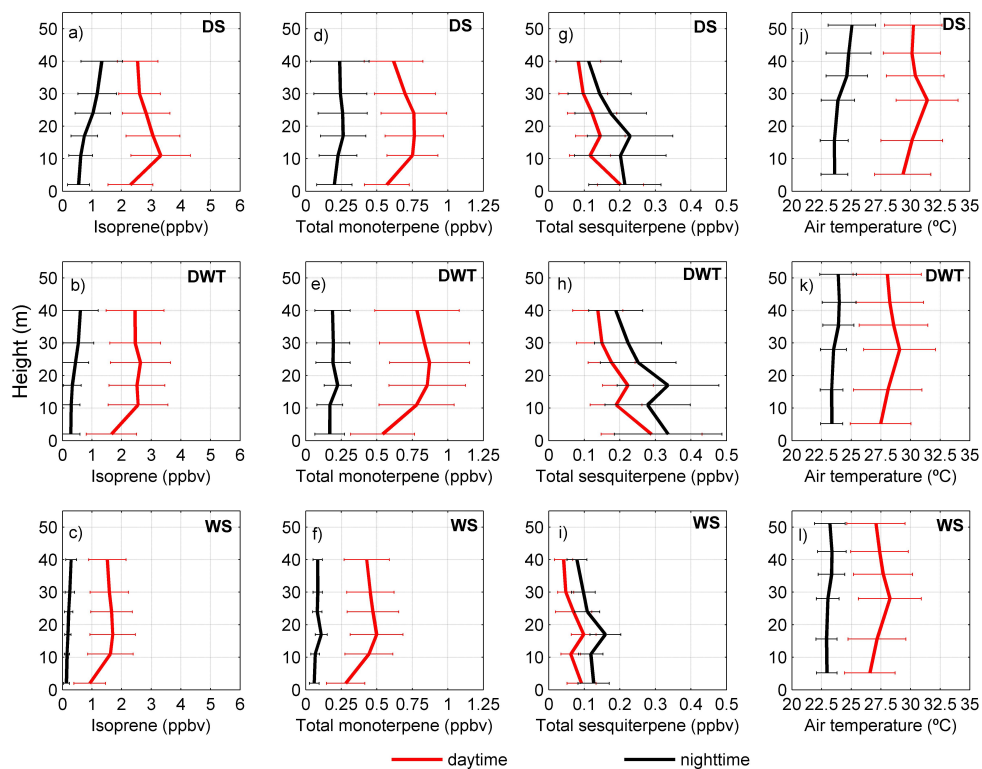


Figure 2: Daytime (10:00-16:00, LT) and nighttime (22:00-04:00, LT) average vertical profiles of isoprene (a, b, c), total monoterpenes (d, e, f), total sesquiterpenes (g, h, i), and air temperature (j, k, l) of the dry season (DS), the dry-to-wet transition season (DWT) and the wet season (WS). Error bars represent one standard deviation.

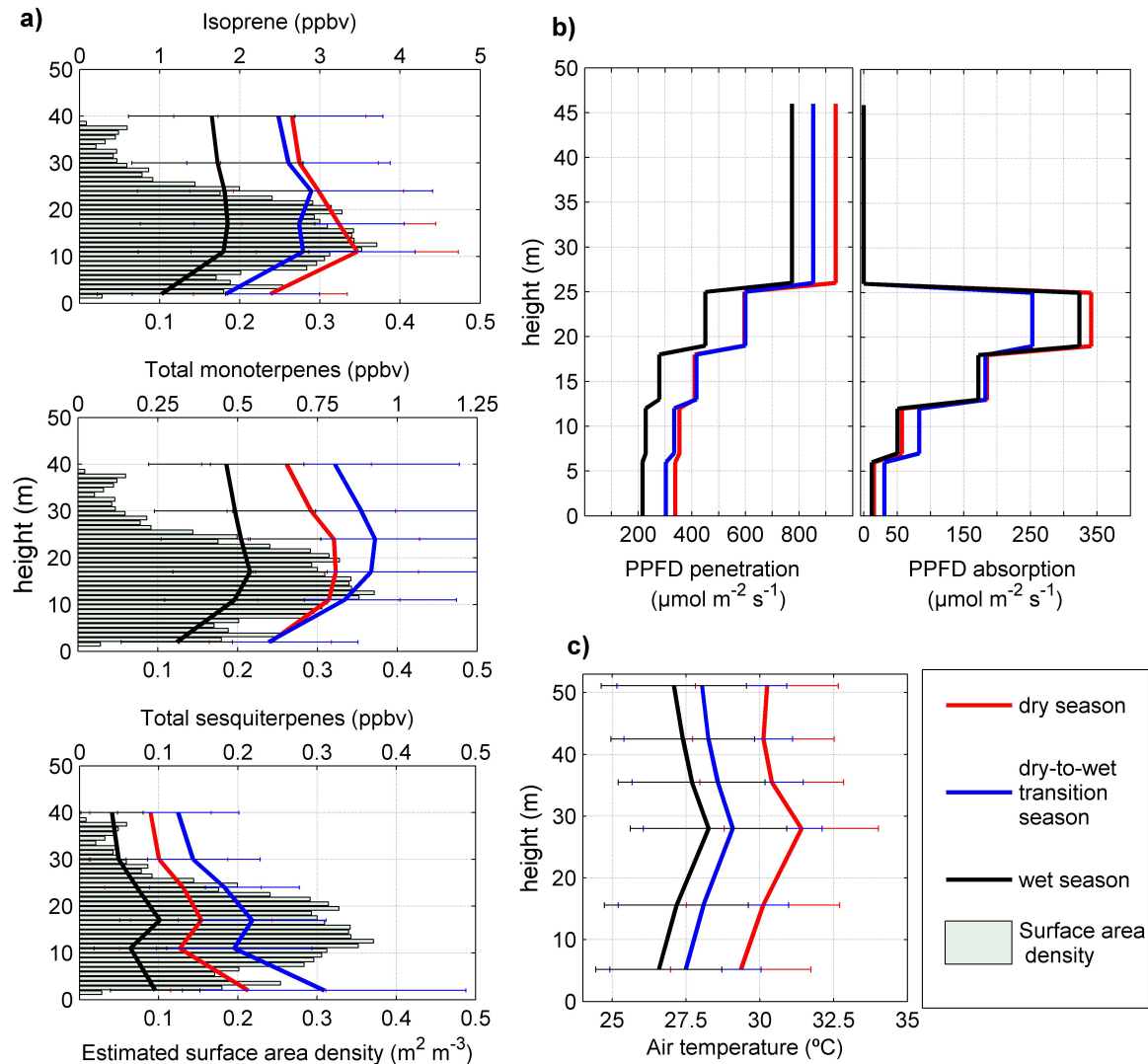


Figure 3: Daytime (10:00-16:00, LT) vertical profiles of mixing ratios of isoprene, total monoterpenes and total sesquiterpenes from the dry season to the wet season; and estimated surface area density of the canopy at this study site (ground-based measurements carried out in March/2004 using LIDAR - Light Detection And Ranging) (Parker and Fitzjarrald, 2004) (a). Vertical profile of photosynthetic photon flux density (PPFD) penetration and absorption by the canopy from the dry season to the wet season modeled by MEGAN 2.1 (b). Daytime (10:00-16:00, LT) air temperature profiles from dry season to wet season measured at K34 tower (c). In fig. 1a the top and the bottom x axis represent isoprenoid mixing ratios and estimated surface area density of the canopy, respectively. Error bars represent one standard deviation.

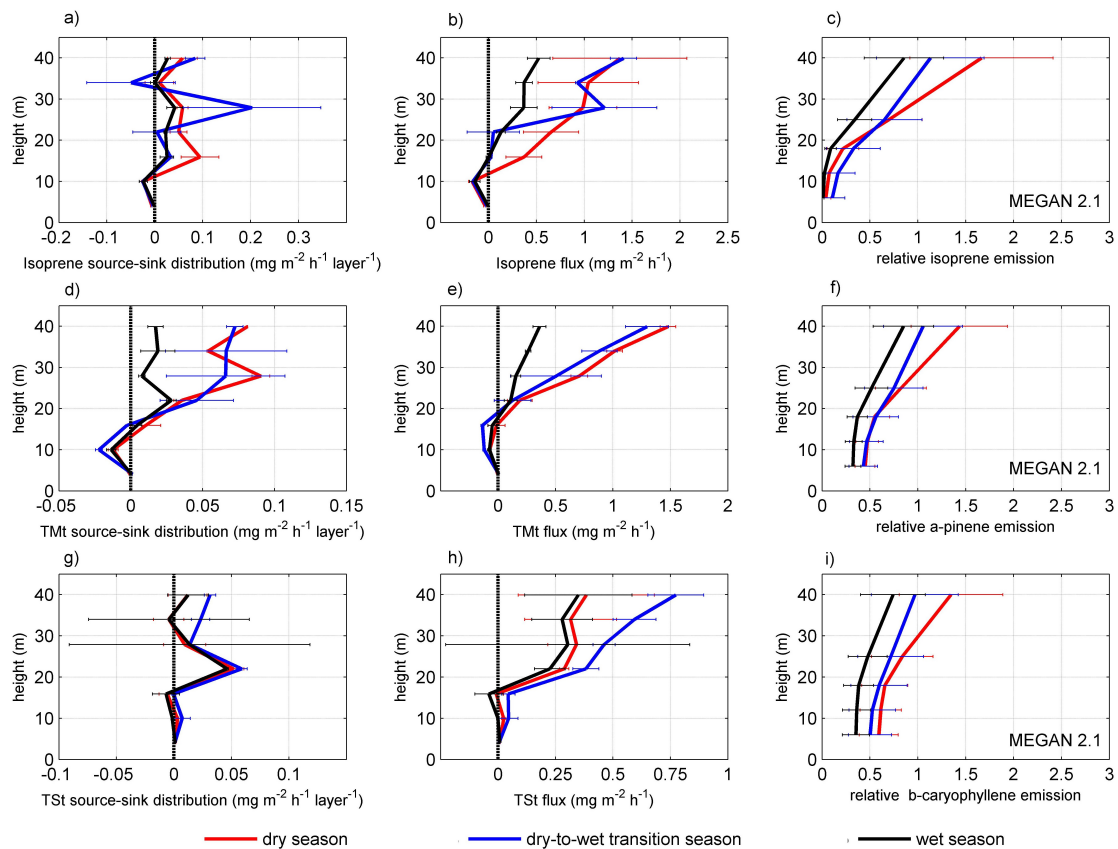


Figure 4: Daytime (10:00-14:00, LT) source-sink distribution inside and above the canopy, cumulative flux estimation, and relative emission modeled by MEGAN 2.1 of isoprene (a, b, c), total monoterpenes (TMt) (d, e, f) and total sesquiterpenes (TSst) (g, h, i) from the dry season to the wet season. Error bars represent one standard deviation.

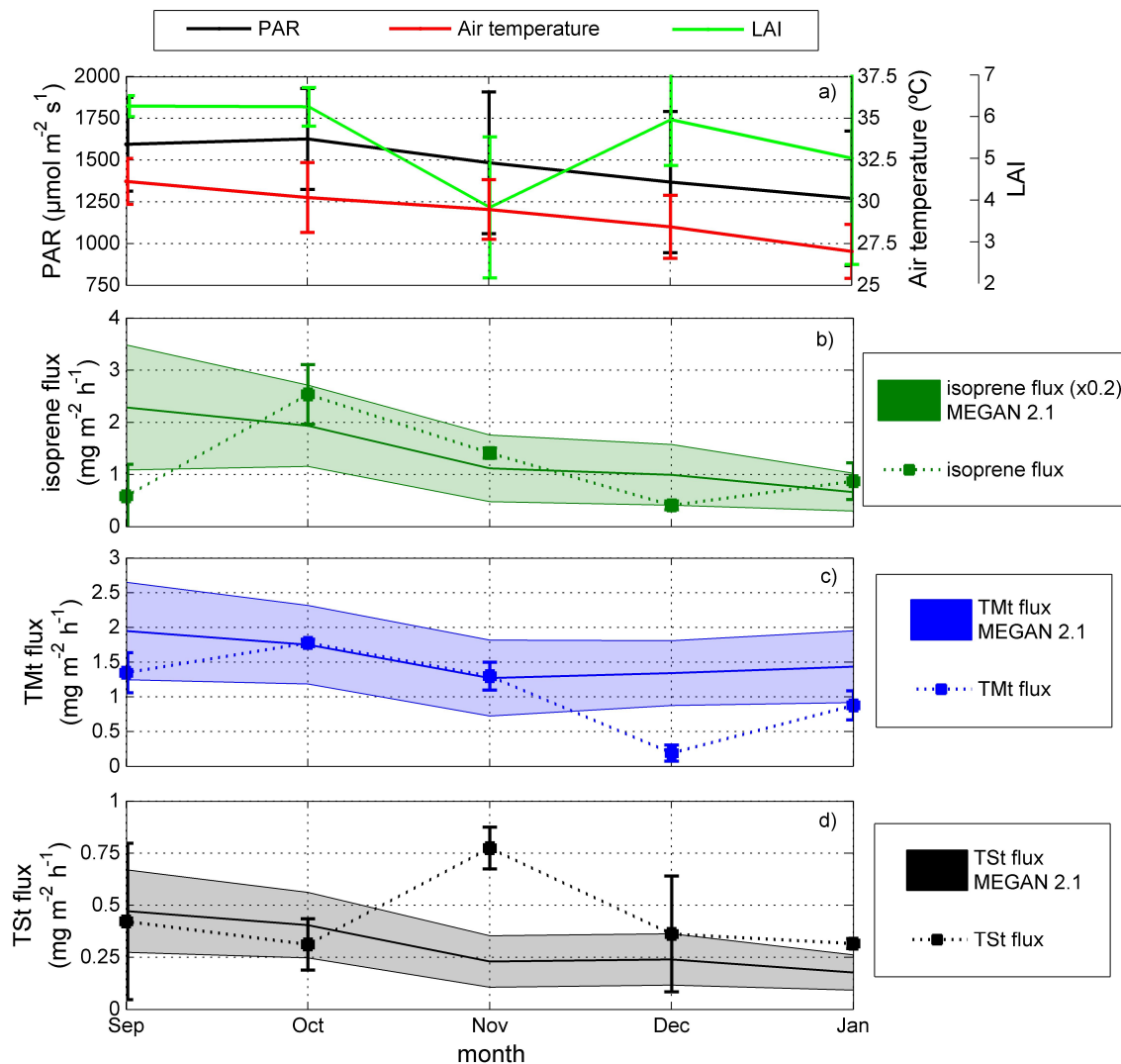


Figure 5: Monthly averages of air temperature and PAR (measured at K34 tower during 10:00-14:00, LT), and LAI (MODIS, 8-day observations) (a). Monthly averages of fluxes of isoprene (b), total monoterpenes (TMt) (c) and total sesquiterpenes (TSt) (d). Flux based on in-situ PTR-MS measurements (inverse Lagrangian transport model - estimates for 10:00-14:00, LT, at TT34 tower) are represented by solid squares and one standard deviation; fluxes modeled by MEGAN 2.1 (estimates for 10:00-14:00, LT) are shown by solid lines and filled areas that represent one standard deviation. Isoprene flux modeled by MEGAN 2.1 in (b) were divided by five. Error bars represent one standard deviation.

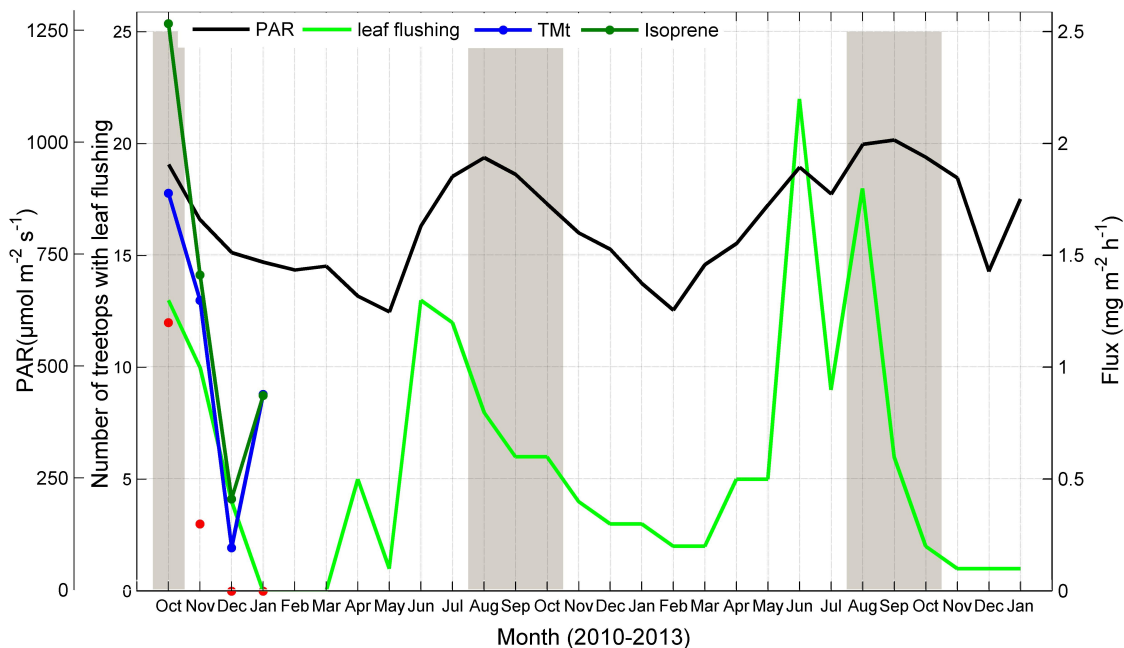


Figure 6: Estimated monthly leaf flushing (light green line) (Tavares, 2013), and monthly average of PAR measured from October 2010 to January 2013 at K34 tower (06:00-18:00, LT) (black line). For the period of this study, leaf flushing is also represented by the analysis of canopy images for every six days from October 2010 to January 2011 (red circles). Monthly averages of fluxes of isoprene (dark green line) and total monoterpenes (blue line) (estimated for 10:00-14:00, LT, at TT34 tower). Grey areas represent the period of the dry season.

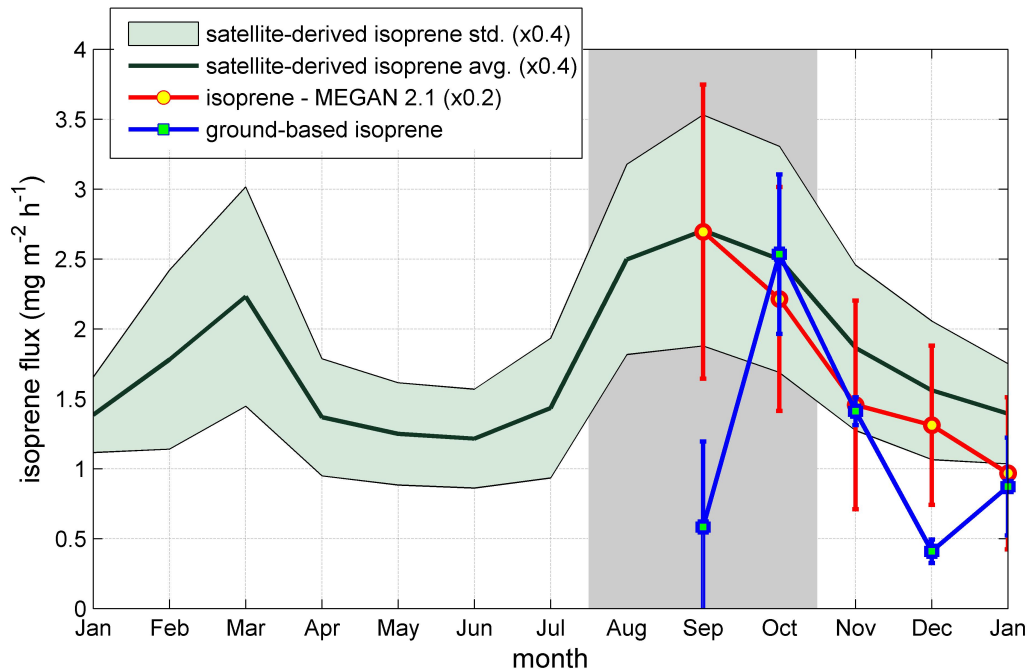


Figure 7: Comparison of monthly isoprene emissions based on in-situ PTR-MS measurements (inverse Lagrangian transport model) and satellite-derived estimates and MEGAN 2.1 estimates. Satellite-derived estimates are from January 2010 to January 2011, and ground-based estimates are from September 2010 to January 2011. Satellite-derived and MEGAN 2.1 estimates were divided by 2.5 and 5, respectively. Grey area represents the period of the dry season. Error bars represent one standard deviation.